Brownian Motion

Reem Mokhtar

What is a Ratchet?

A device that allows a shaft to turn only one way

http://www.hpcgears.com/products/ratchets_pawls.htm

Feynman, R. P., Leighton, R. B., & Sands, M. L. (1965). *The Feynman Lectures on Physics: Mechanics, radiation, and heat* (Vol. 1). Addison-Wesley.

Thermodynamics

2nd law, by Sadi Carnot in 1824.

- Zeroth: If two systems are in thermal equilibrium with a third system, they must be in thermal equilibrium with each other.
- First: Heat and work are forms of energy transfer.
- **Second: The entropy of any isolated system not in thermal equilibrium almost always increases.**
- Third: The entropy of a system approaches a constant value as the temperature approaches zero.

http://en.wikipedia.org/wiki/Laws_of_thermodynamics

Why is there a maximum amount of work that can be extracted from a heat engine?

- Why is there a maximum amount of work that can be extracted from a heat engine?
- Carnot's theorem: heat cannot be converted to work cyclically, if everything is at the same temperature → Let's try to negate that.

The Ratchet As An Engine

Ratchet, pawl and spring.

Let us try to invent a device which will violate the Second Law of Thermodynamics, that is, a gadget which will generate work from a heat reservoir with everything at the same temperature. Let us say we have a box of gas at a certain temperature, and inside there is an axle with vanes in it. (See Fig. 46–1 but take

First, our idealized ratchet is as simple as possible, but even so, there is a pawl, and there must be a spring in the pawl. The pawl must return after coming off a tooth, so the spring is necessary.

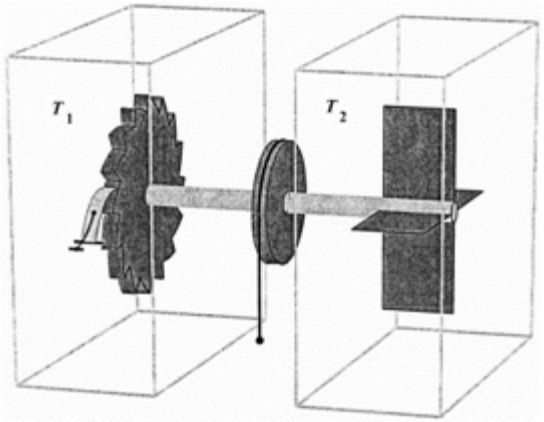

The Ratchet As An Engine

Forward rotation

ε	energy to lift the pawl
$L\theta$	work done on load
$\varepsilon + L\theta$	energy to rotate wheel by one tooth
$f_B^f = Z^{-1} e^{-(\varepsilon + L\theta)/\tau_1}$	Boltzmann factor for work provided by vane
νf_B^f	ratching rate with ν attempt frequency
$\nu f_B^f L\theta$	power delivered

ε energy provided to ratchet

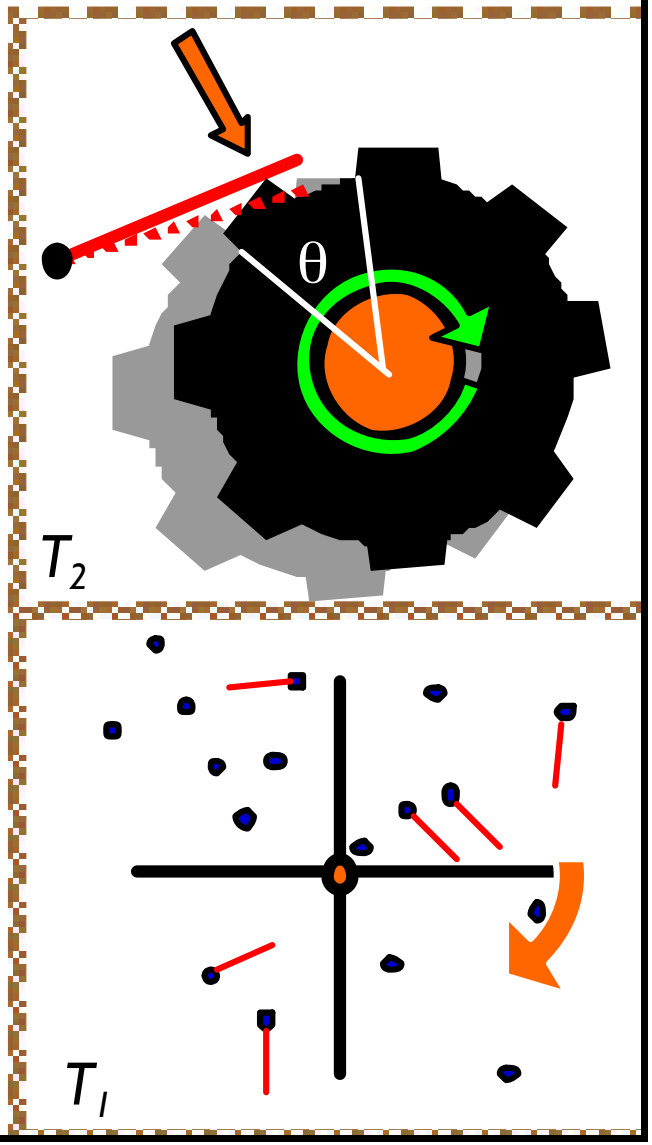

Backward rotation

ε	energy to lift the pawl
$L\theta$	work provided by load
$\varepsilon + L\theta$	energy given to vane
$f_B^b = Z^{-1} e^{-\varepsilon/\tau_2}$	Boltzmann factor for tooth slip
νf_B^b	slip rate with attempt frequency ν

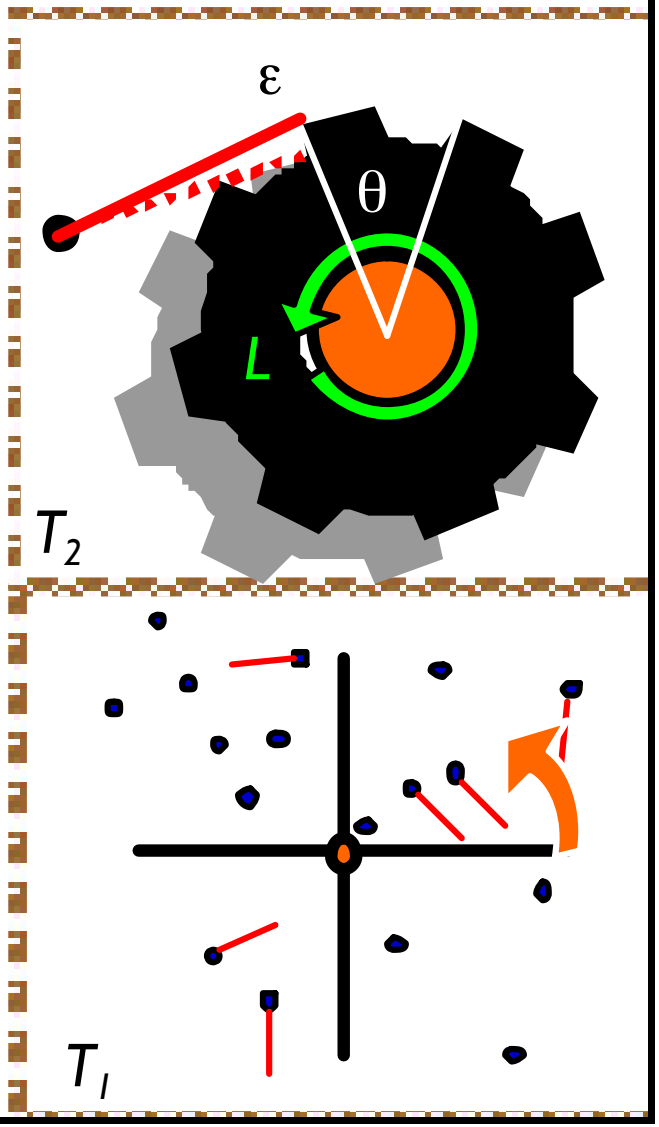

Equilibrium and reversibility

ratching rate = slip rate $\quad f_B^b = f_B^f$

$$L_{eq}\theta = \left(\frac{\tau_1}{\tau_2} - 1\right)\varepsilon$$

Reversible process by increasing the load infinitesimally from equilibrium L_{eq}. This forces a rotation leading to heating of reservoir 1 with $dq_1 = \varepsilon + L_{eq}$? and cooling of reservoir 2 as $dq_2 = -\varepsilon$:

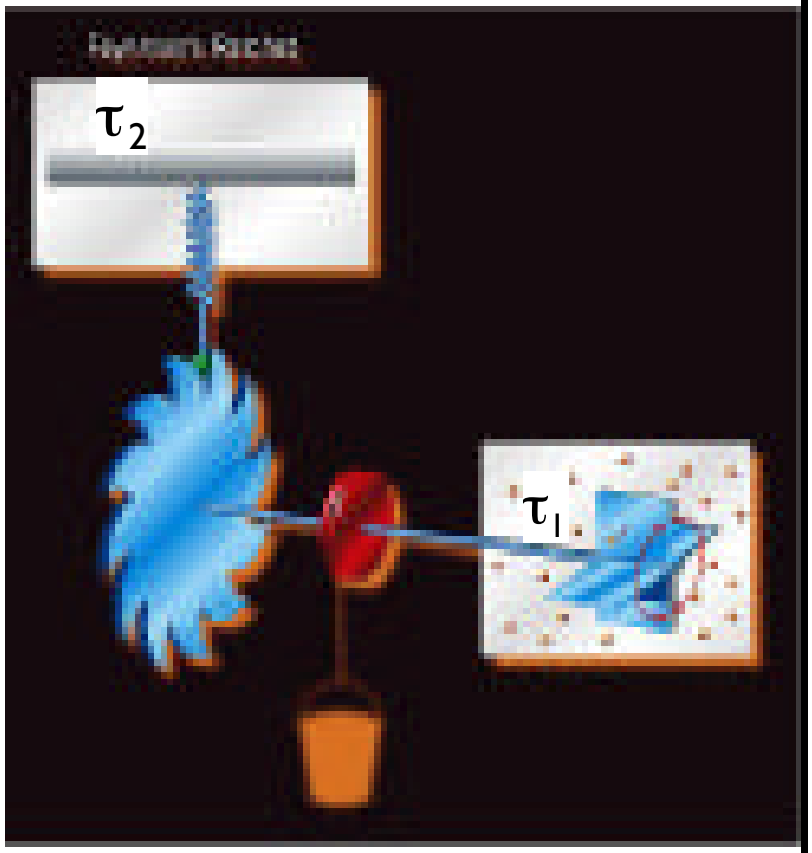

$$\frac{dq_1}{-dq_2} = \frac{\varepsilon + L_{eq}\theta}{\varepsilon} = \frac{\tau_1}{\tau_2}$$

$$\frac{dq_1}{\tau_1} + \frac{dq_2}{\tau_2} = dS_1 + dS_2 = 0$$

isentropic process

Ratchet Brownian motor

Angular velocity of ratchet: $\Omega = \theta\nu\left(f_B^f - f_B^b\right) = \theta\nu\left(e^{-\frac{\varepsilon + L\theta}{\tau_1}} - e^{-\frac{\varepsilon}{\tau_2}}\right)$

Without load: $\Omega \xrightarrow{L=0} \theta\nu\left(e^{-\frac{\varepsilon}{\tau_1}} - e^{-\frac{\varepsilon}{\tau_2}}\right)$

Equal temperatures: $\Omega(L) \xrightarrow{\tau_1=\tau_2=\tau} \theta\nu\, e^{-\frac{\varepsilon}{\tau}}\left(e^{-\frac{L\theta}{\tau}} - 1\right)$

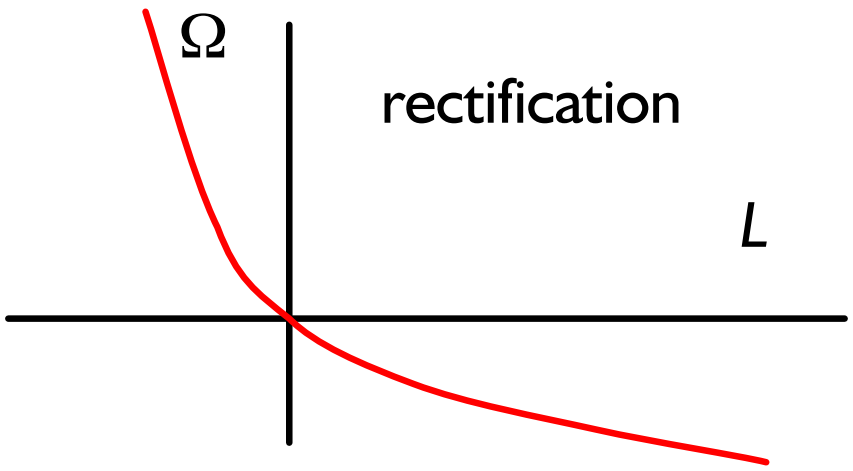

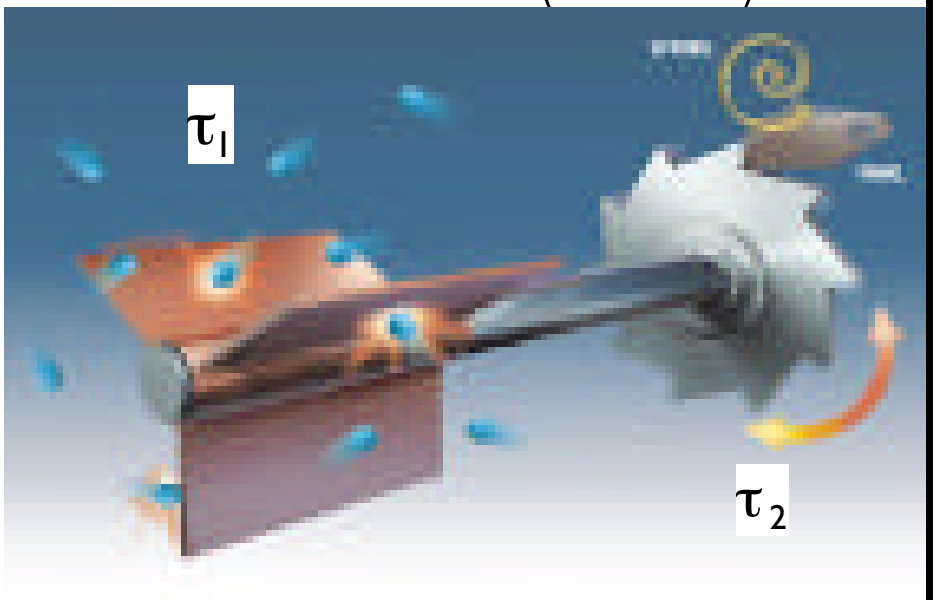

Kinesin

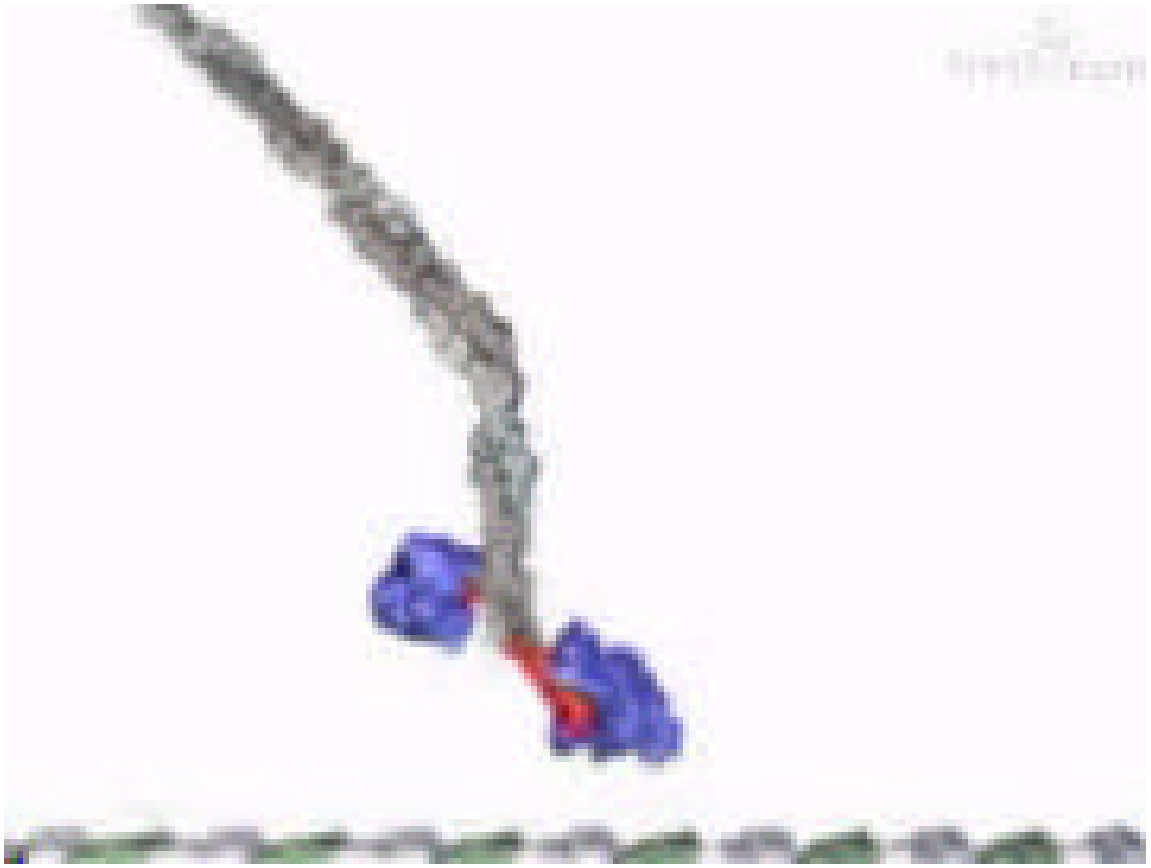

The two heads of the kinesindimer work in a coordinated manner to move processivelyalong the microtubule. The catalytic core (blue) is bound to a tubulinheterodimer (green, b-subunit; white, asubunit) along a microtubule protofilament (the cylindrical microtubule is composed of 13protofilament tracks). In solution, both kinesinheads contain ADP in the active site (ADP release is ratelimiting in the absence of microtubules). The chaotic motion of the kinesinmolecule reflects Brownian motion. One kinesinhead makes an initial weak binding interaction with the microtubule and then rearranges to engage in a tight binding interaction. Only one kinesinhead can readily make this tight interaction with the microtubule, due to restrai nts imposed by the coiled -coil and pre-stroke conformation of the neck linker in the bound head. Microtubule binding releases ADP from the attached head. ATP then rapidly enters the empty nucleotide bind ing site, which triggers the neck linker to zipper onto the catalyti ccore (red to yellow transition). This action throws the detached head forward and allows it to reach the next tubulinbinding site, thereby creating a 2-head -bound intermediate in which the neck linkers in the trailing and leading heads are pointing forward (post-stroke; yellow) and backwards (pre-stroke; red) respectively. The trailing head hydrolyzes the ATP (yellow flash of ADP -Pi), and reverts to a weak microtubule binding state (indicated by the bouncing motion) and releases phosphate (fading Pi). Phosphate release also causes the unzippering of the neck linker (yellow to red transition). The exact timing of the strongto-weak microtubule binding transition and the phosphate release step are not well-defined from current experimental data. During the time when the trailing head execut es the previously described actions, the leading head releases ADP, binds ATP, and zippers its neck linker onto the catalytic core. This neck linker motion throws the trailing head forward by 160 Å to the vicinity of new tubulinbinding site. After a random diffusional search, the new lead head docks tightly onto the binding site which comp letes the 80 Å step of the motor. The movie shows two such 80 Å steps of the kinesinmotor. The surface features of the kinesin motor domains and the microtubule protofilament were rendered from X -ray and EM crystallographic structures by Graham Johnson (fiVth media: www.fiVth.com) using the programs MolView, Strata Studio Pro and Cinema 4D. PDB files used were human conventional kinesin (prestroke, red: #1BG2) and rat conventional kinesin(poststroke, yellow: #2KIN). In human conventional kinesin, the neck linker is mobile and its located in the prestrokestate is estimated from cryo - electron microscopy data. Transitions between states were performed by performing computer-coordinated extrapolations between the prestrokeand poststroke positions. The durations of the events in this sequence were optimized for clarity and do not necessarily reflect the precise timing of events in the ATPasecycle.

Molecular gears

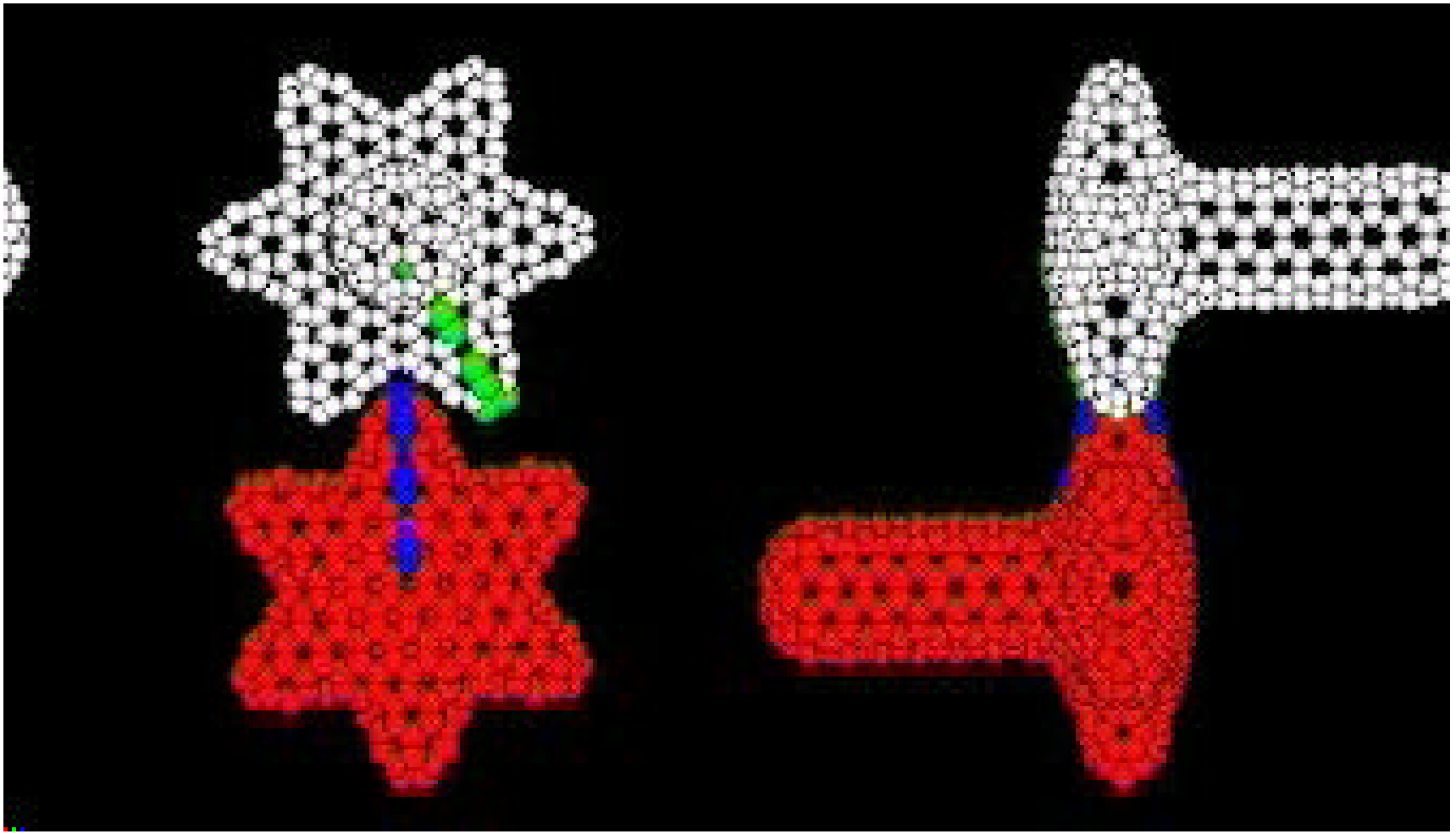

http://chem.iupui.edu/Research/Robertson/Robertson.html#Gears

Diffusion in asymmetric potentials

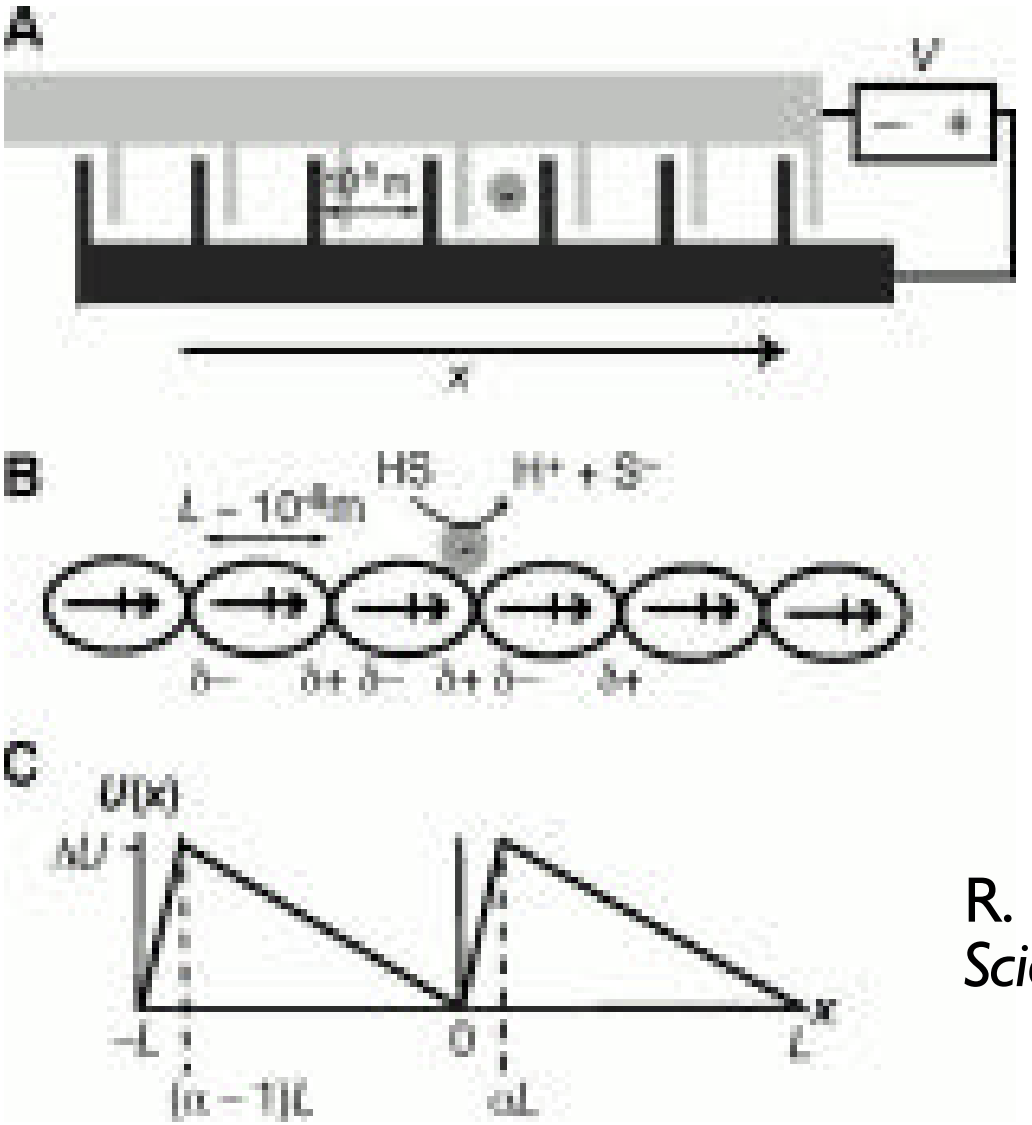

electrostatic potential

chemical potential

R. Dean Astumian,
Science 1997 **276**: 917-922.

Driven Brownian ratchets

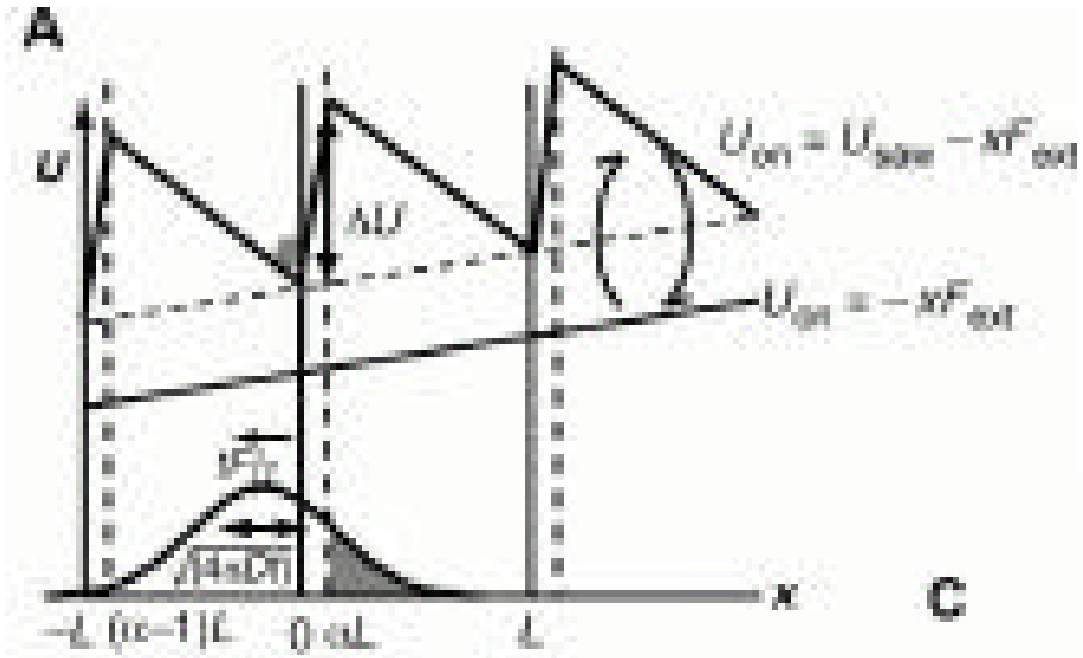

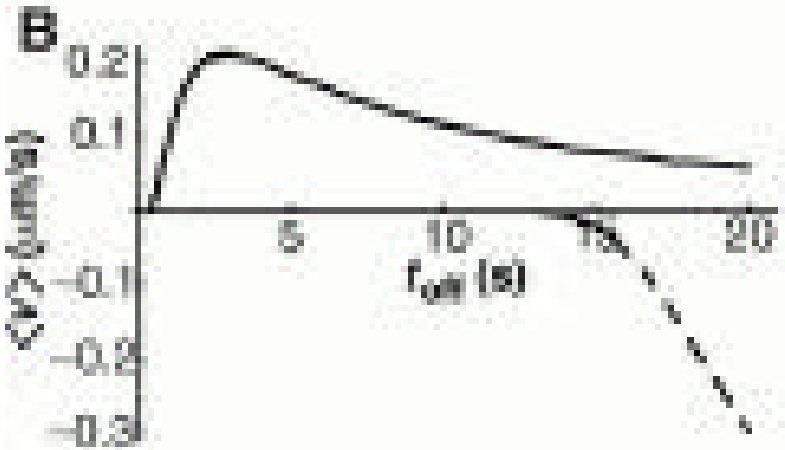

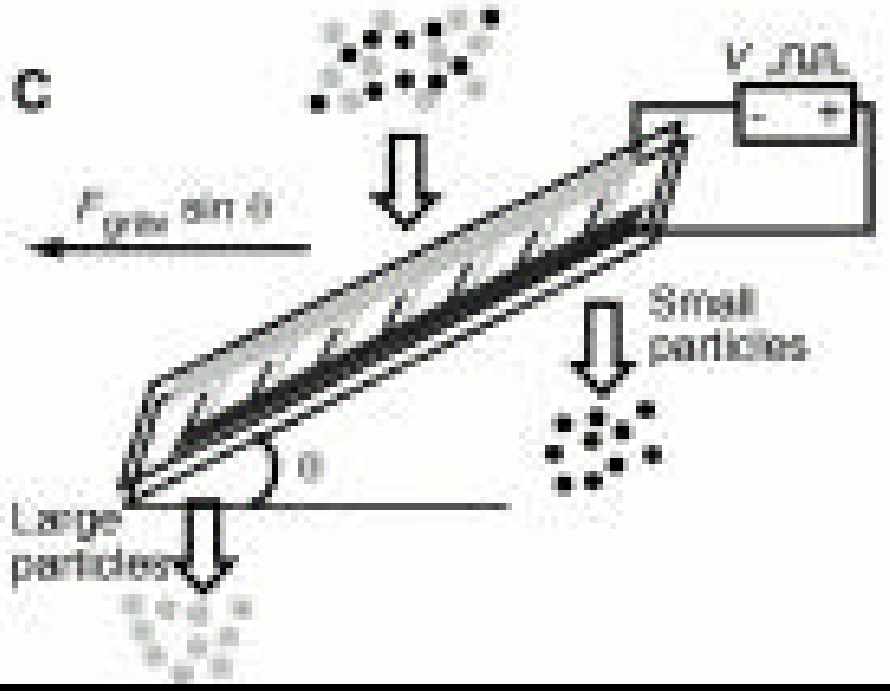

DNA transport by a micromachined Brownian ratchet device

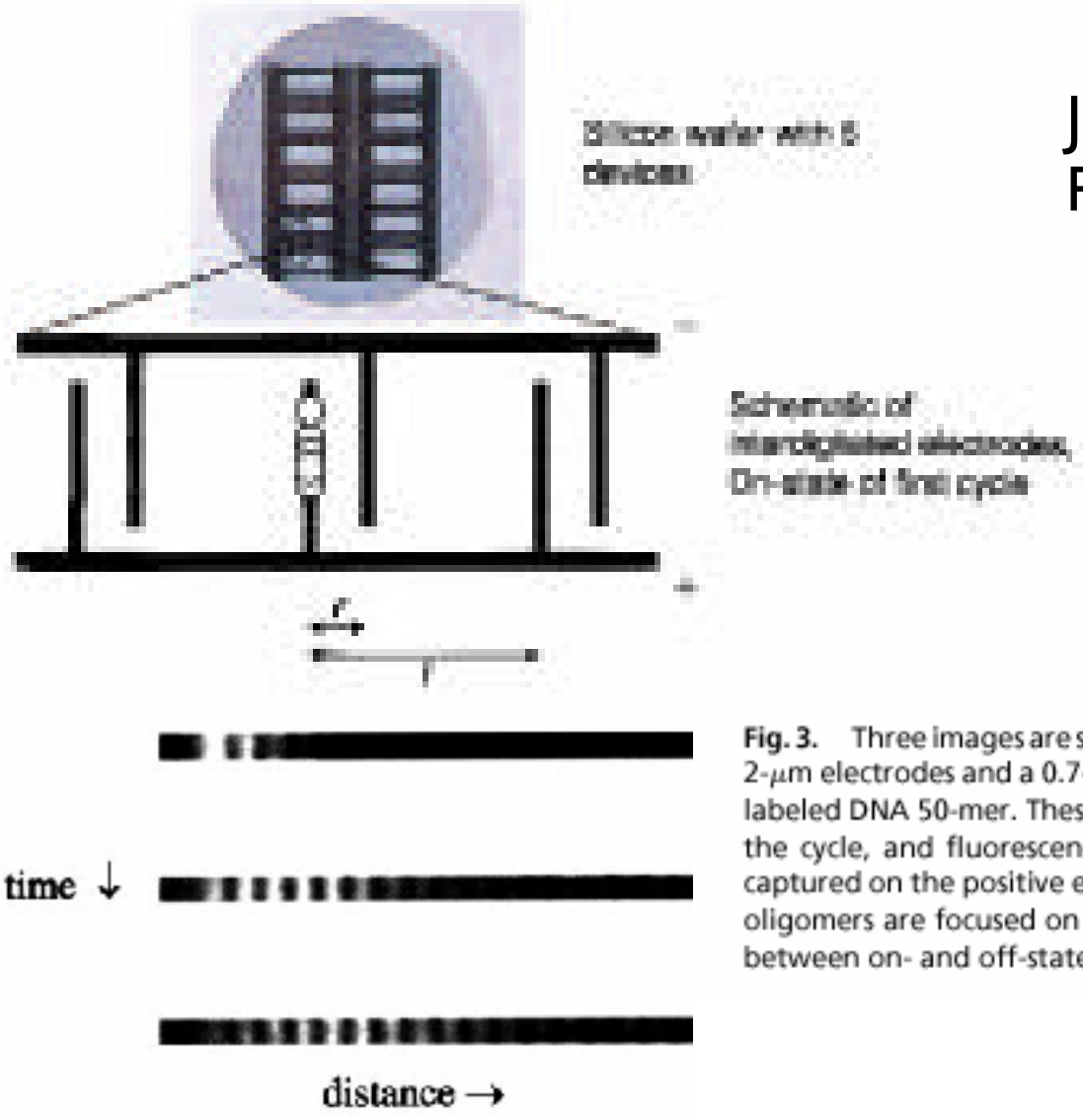

Joel S. Bader *et al.*,
PNAS **96.** 13165 (1999)

Fig. 3. Three images are shown from a typical experiment using a device with 2-μm electrodes and a 0.7-Hz switching frequency to transport a rhodamine-labeled DNA 50-mer. These images were saved during the trapping phase of the cycle, and fluorescence maxima are clearly seen from DNA molecules captured on the positive electrodes. At the start of the experiment, the DNA oligomers are focused on left-most three electrodes. As the potential cycles between on- and off-states, the packet moves to the right and broadens.

Geometrical Brownian ratchet I

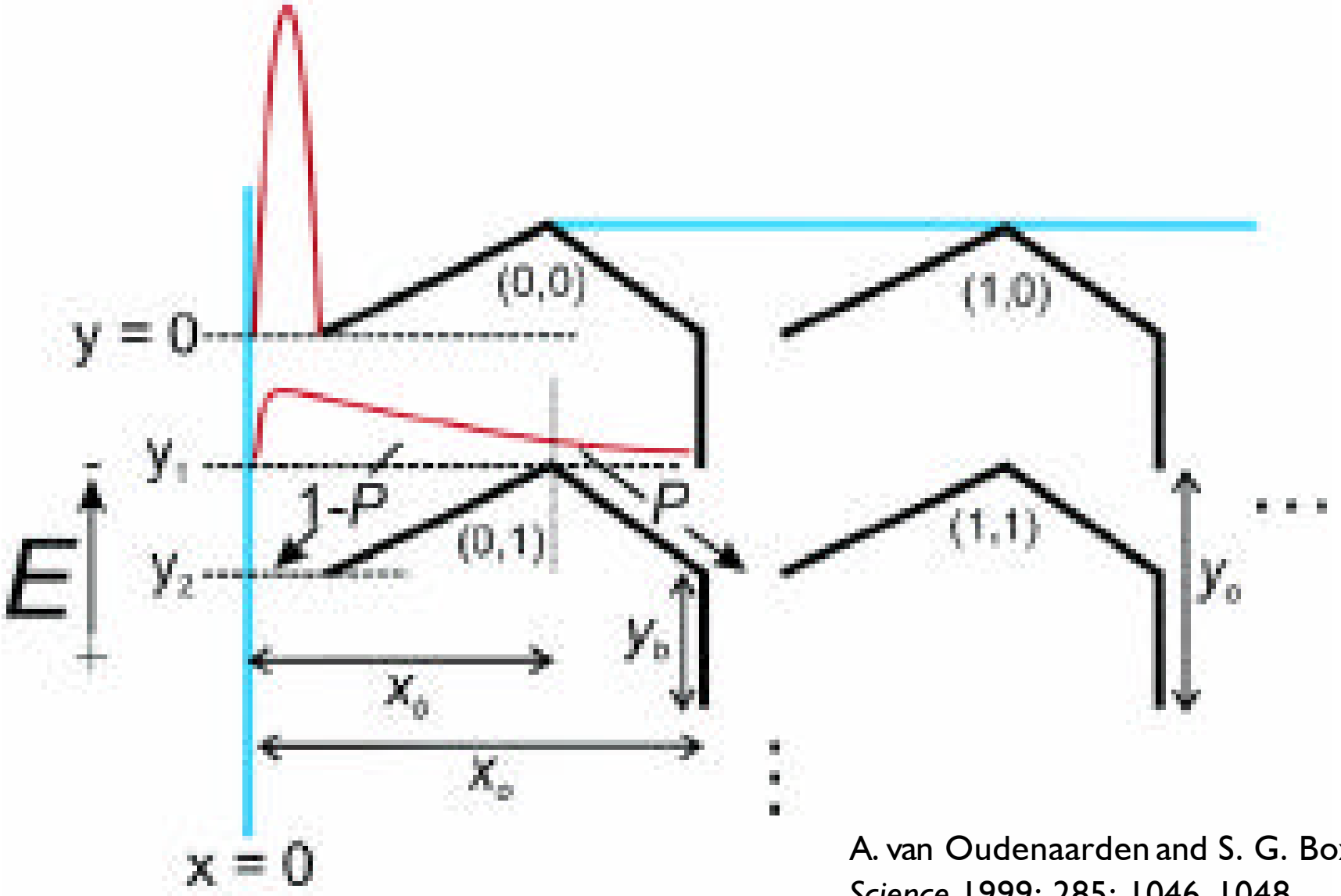

A. van Oudenaarden and S. G. Boxer, *Science* 1999; 285: 1046-1048.

Geometrical Brownian ratchet II

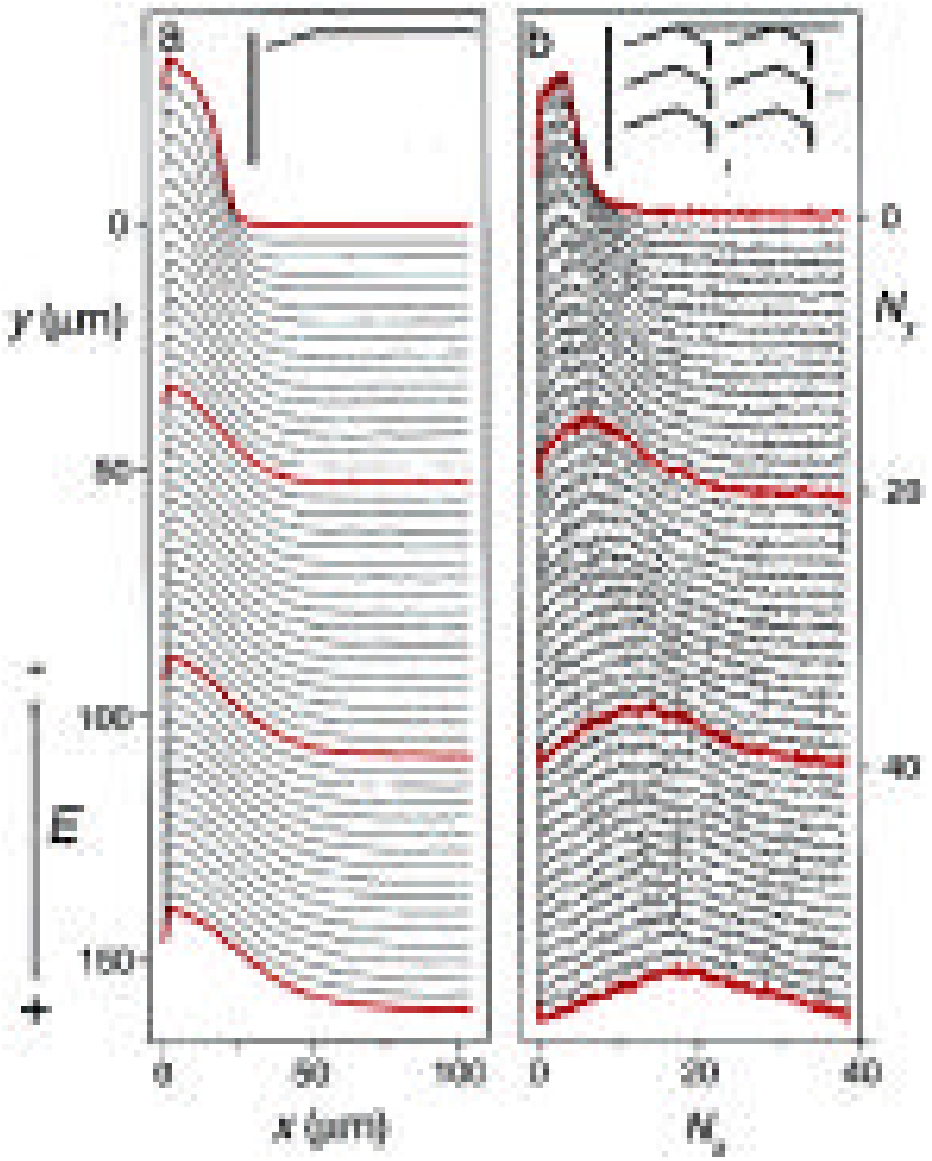

Unidirectional molecular rotation

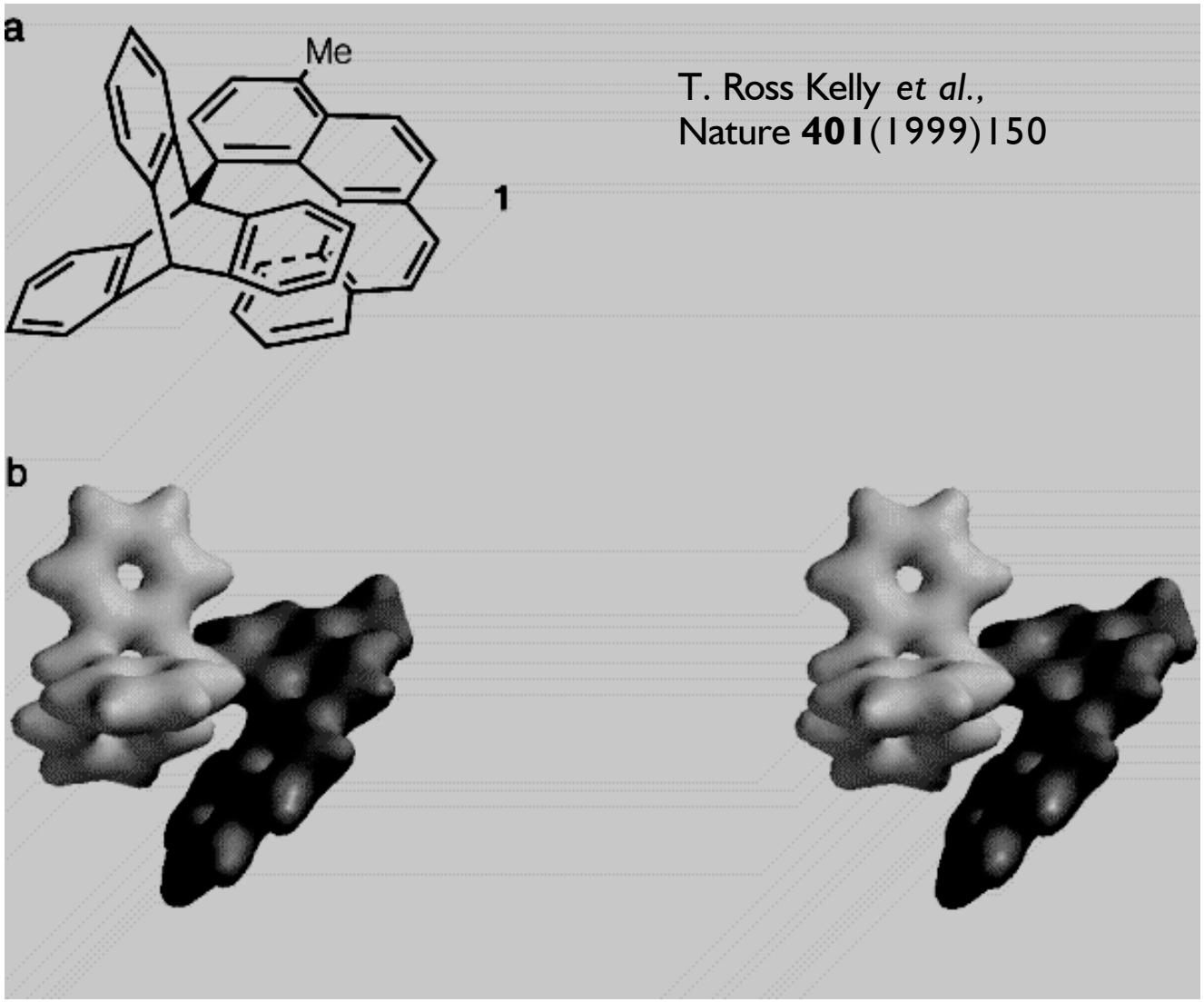

T. Ross Kelly *et al.*,
Nature **401**(1999)150

Chemically driven rotation

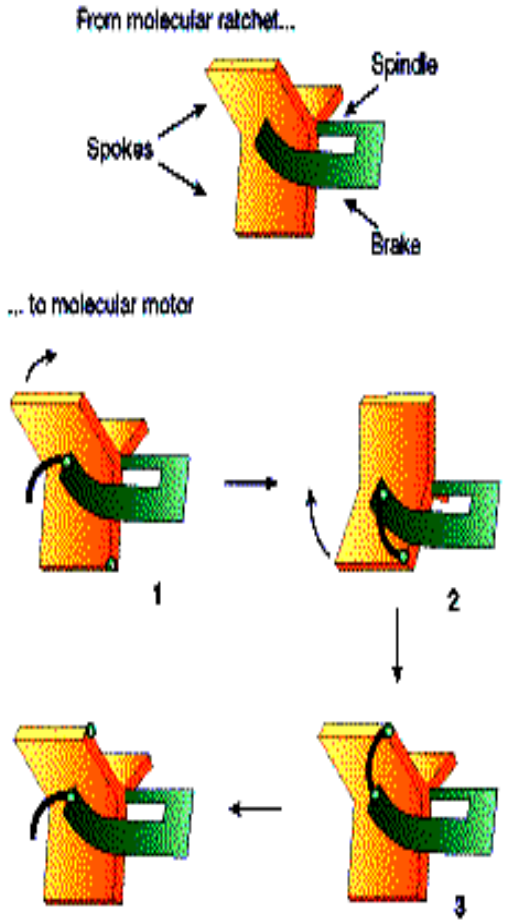

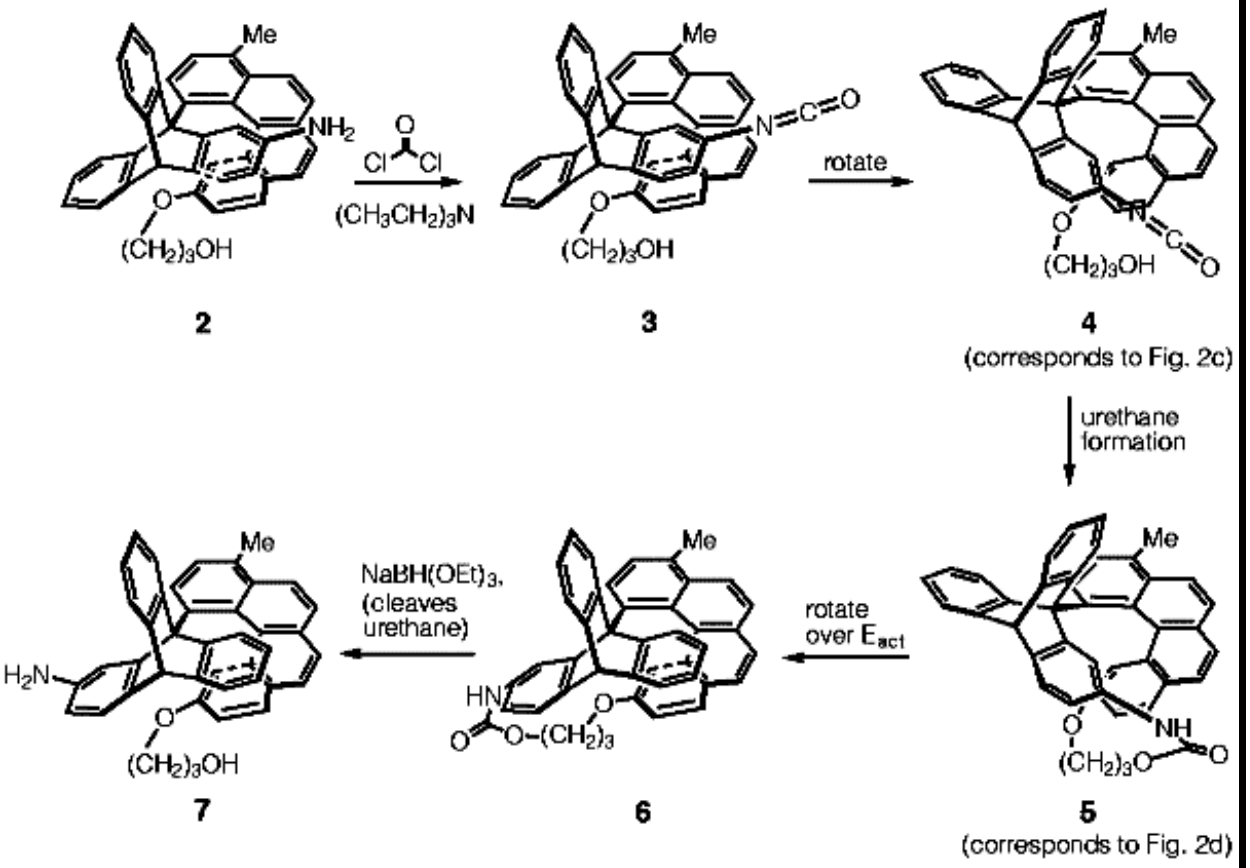

Light driven rotation

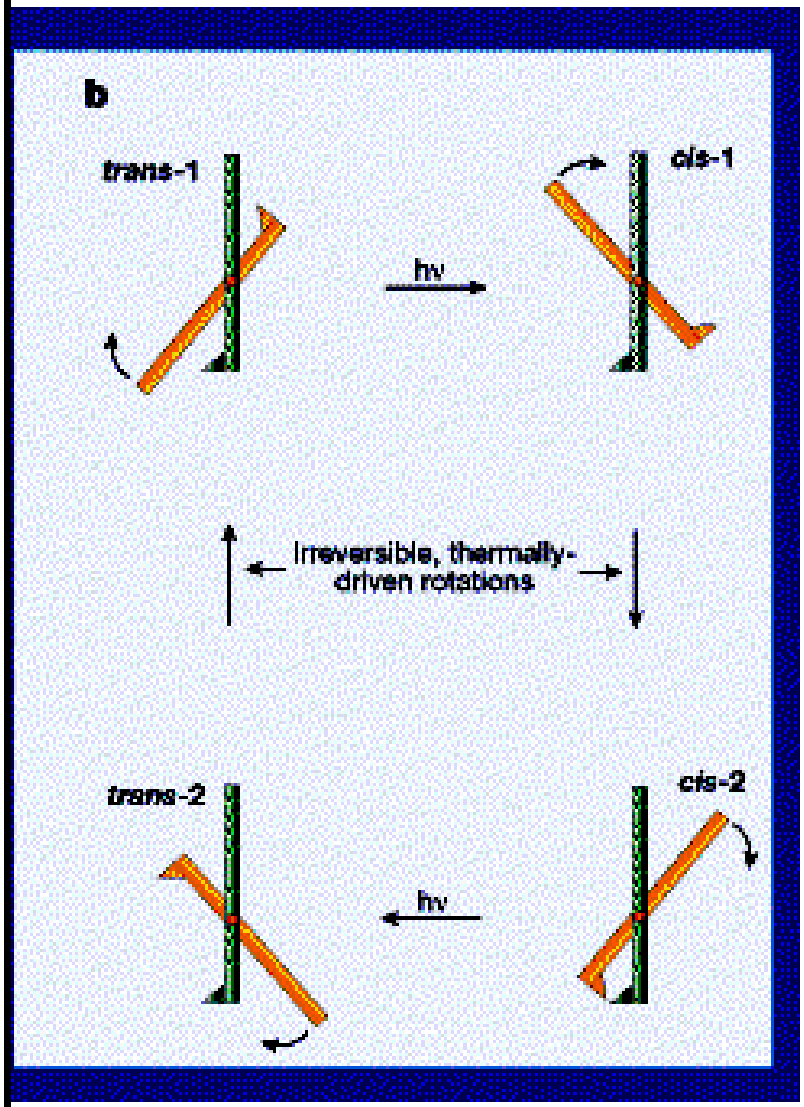

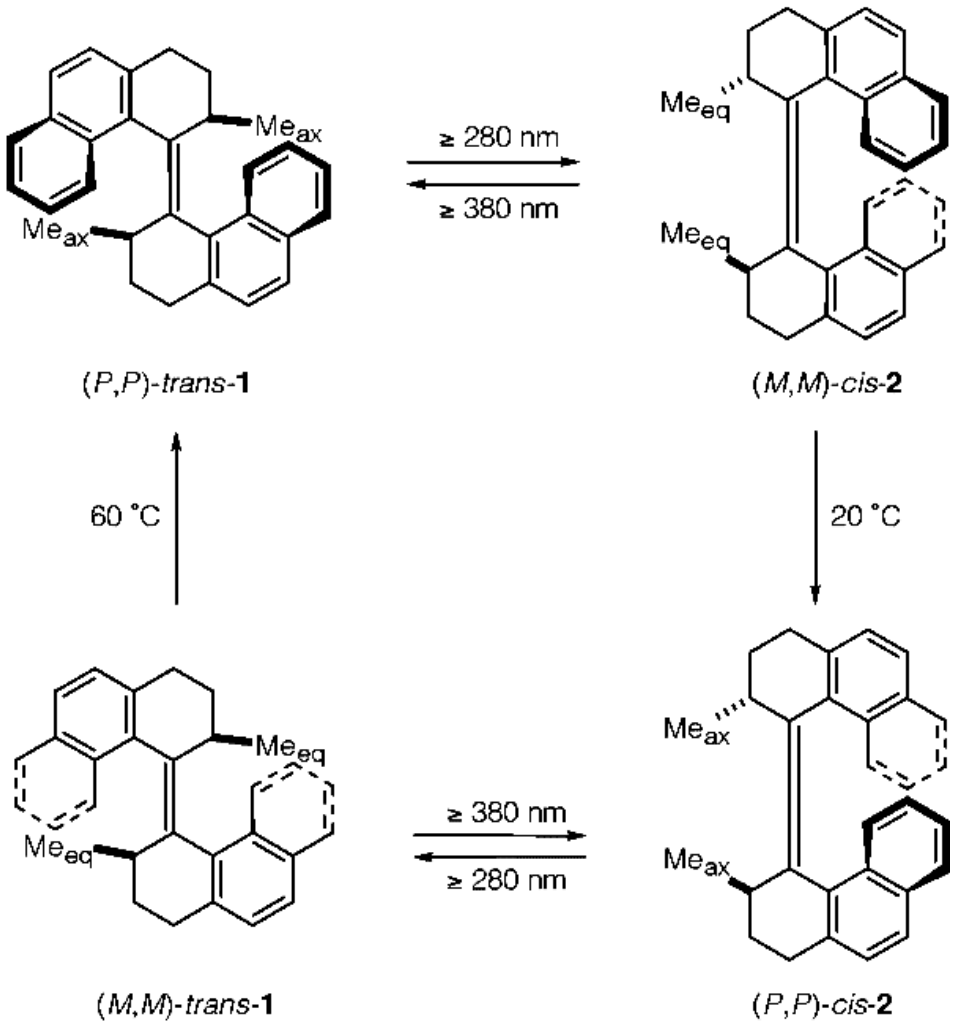

N. Koumura *et al*., Nature **401**(1999)152

Maxwell's demon

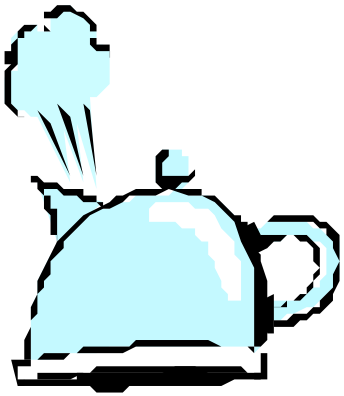

W. Smoluchowski (1941):
No automatic, permanently effective perpetual motion machine van violate the second law by taking advantage of statistical fluctuations (Feynman: the demon is getting hot). Such device might perhaps function if operated by intelligent beings.

W.H. Zurek, Nature **341**(1989)119:
The second law is safe from intelligent beings as long as their abilities to process information are subject to the same laws as these of universal Turing machines.

Quantum demon? (ask Milena Grifoni)

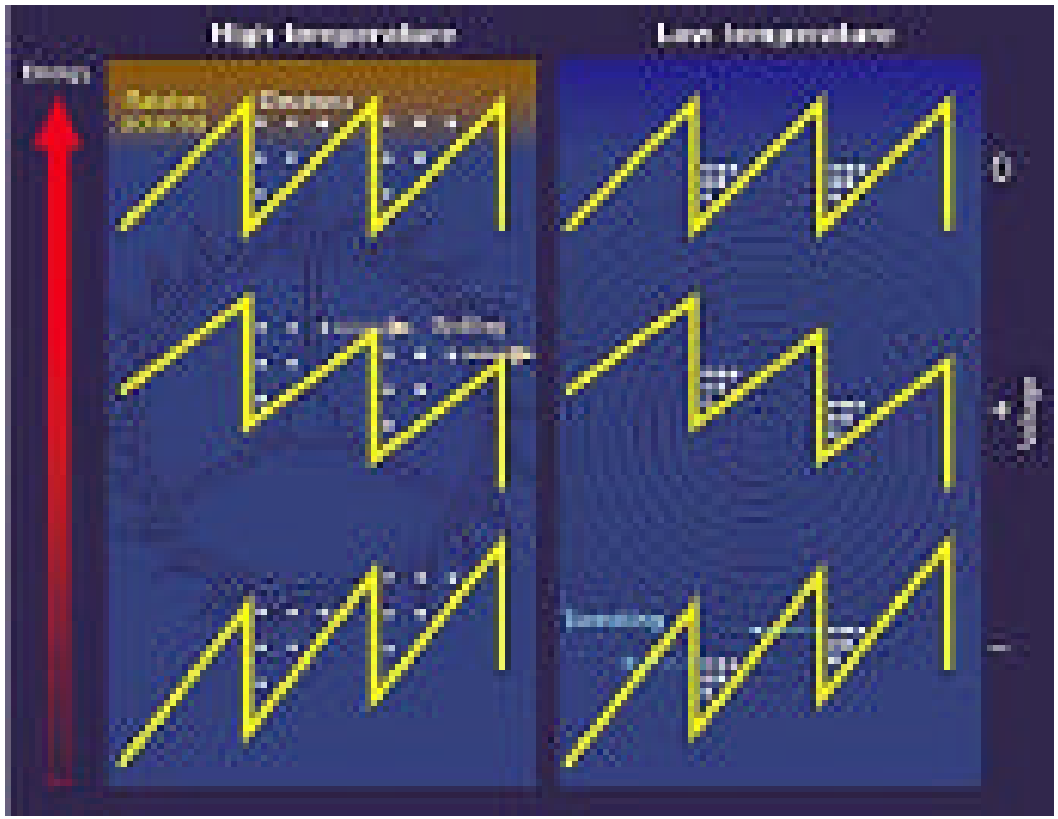

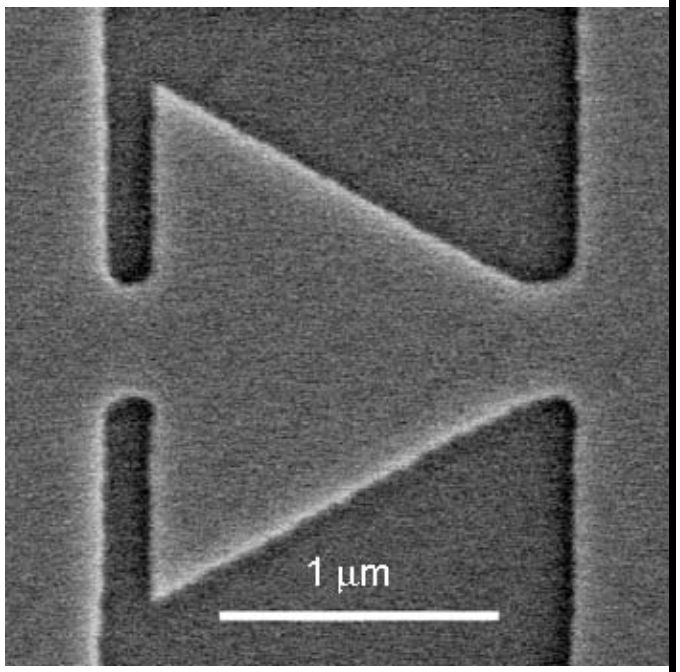

Fluctuations of μm-sized trapped colloidal particles

G.M. Wang *et al.*, Phys. Rev. Lett. 89(2002)050601

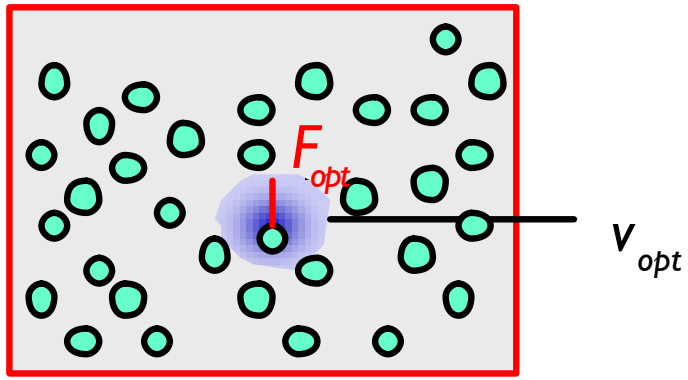

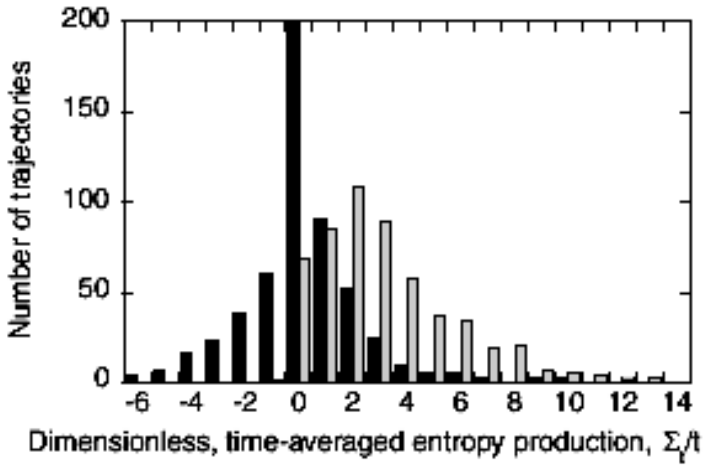

FIG. 1 (color online). Histogram of the dimensionless, time-averaged entropy production, Σ_t/t, from 540 experimental trajectories of a colloidal particle in an optical trap at times $t = 10^{-2}$ (black bars) and $t = 2.0$ (gray bars) seconds after initiation of stage translation. The bin size is $\Delta\Sigma_t/t = 1.0$.

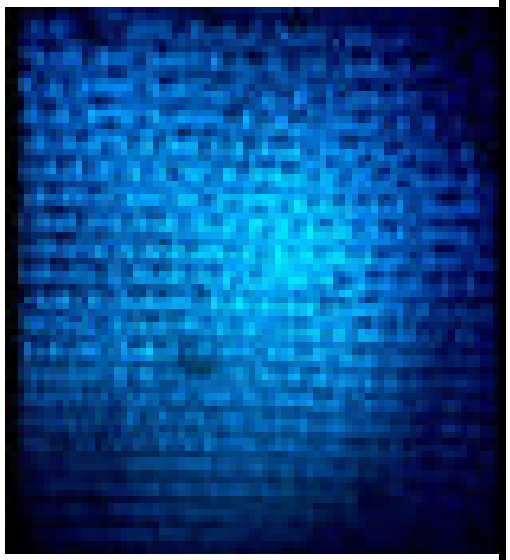

physics.okstate.edu/ackerson/vackerson/

$$\Sigma_t = \frac{1}{\tau}\int_0^t v_{opt}\cdot F_{opt}(s)\,ds$$

Entropy production

The Feynman Thermal Ratchet

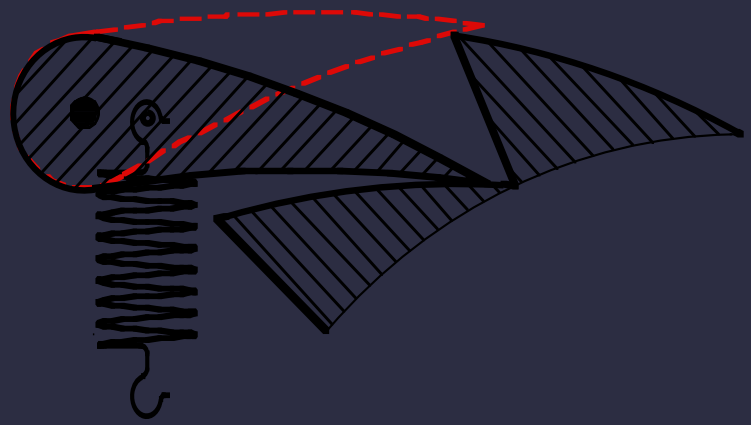

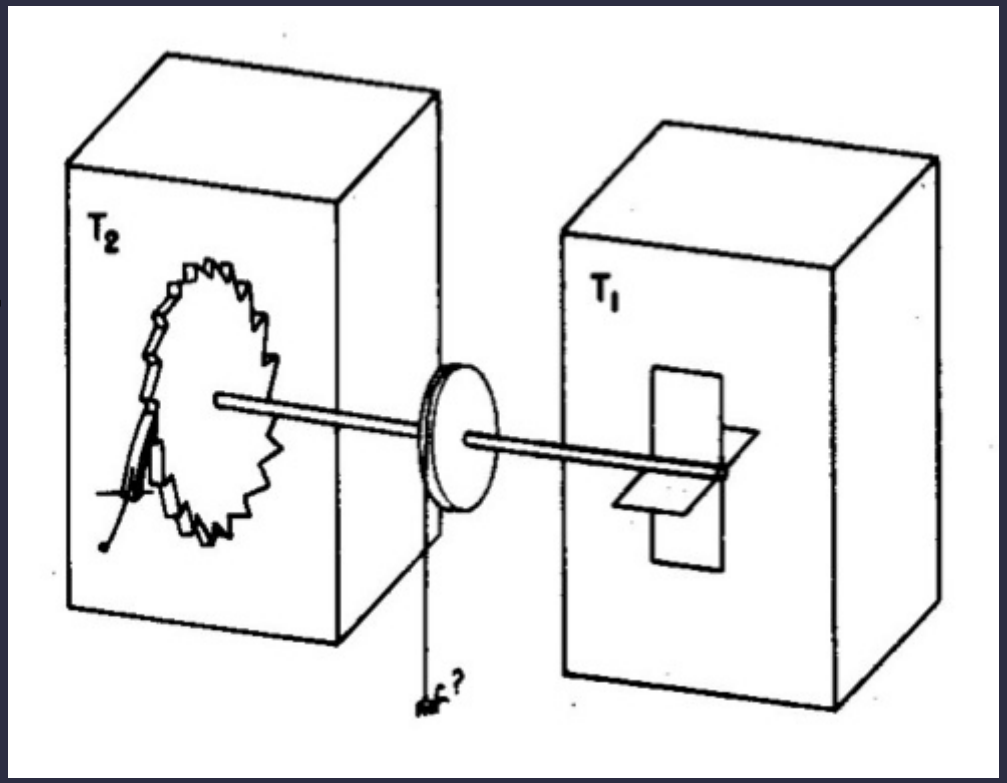

$P_{forward} \sim \exp(-\Delta\varepsilon/kT_1)$
$P_{backward} \sim \exp(-\Delta\varepsilon/kT_2)$

works only if $T_1 > T_2$!!

$$\tau_{rel} \approx Cl^2/(4\pi^2\kappa)$$

motor protein conformational change: *μs*
decay of temperature gradient over 10 nm: ns

➡ wrong model

Brownian Ratchet

(A.F. Huxley ‘57)

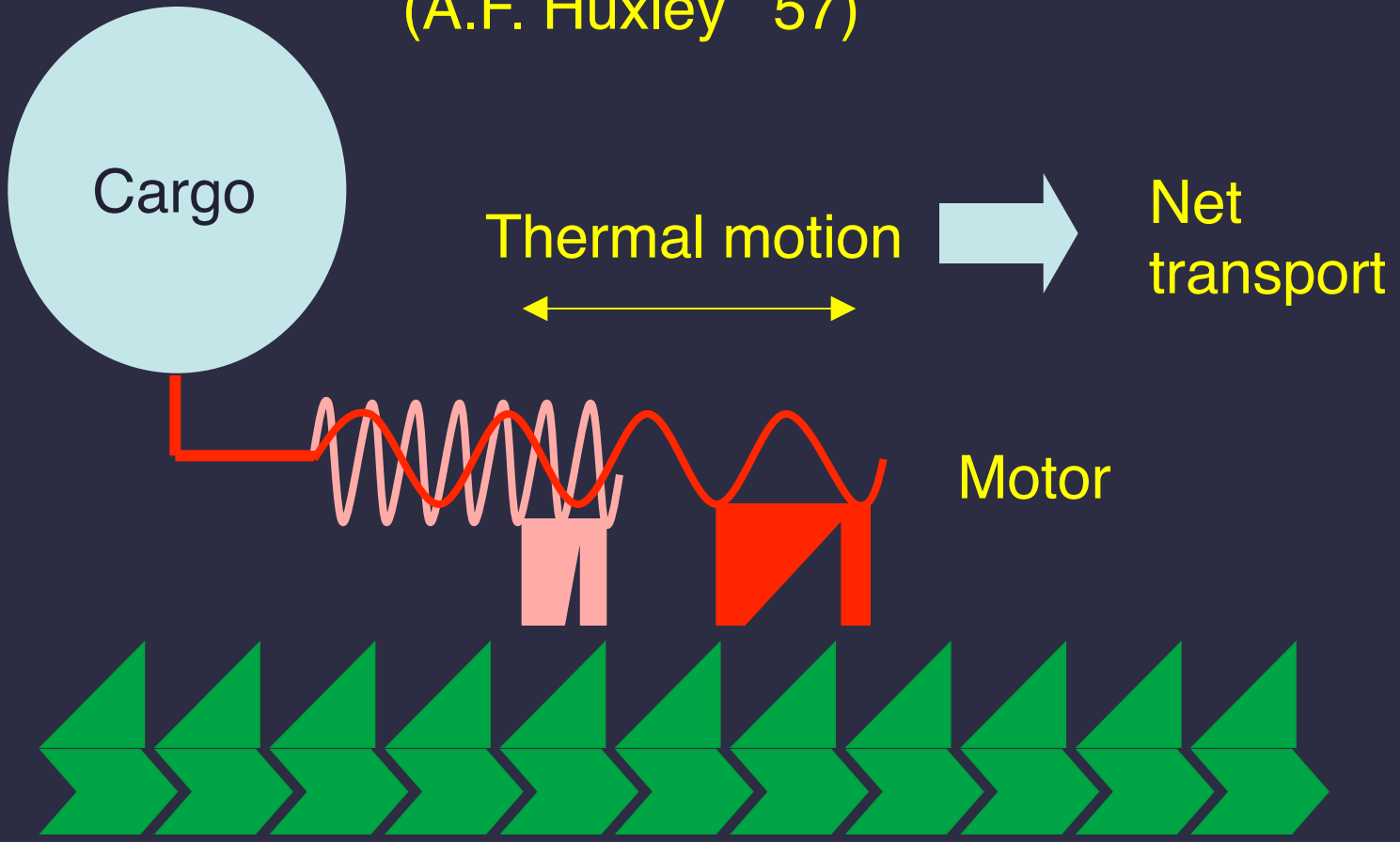

perpetuum mobile? Not if ATP is used to switch the off-rate.

Three-bead assay with ncd

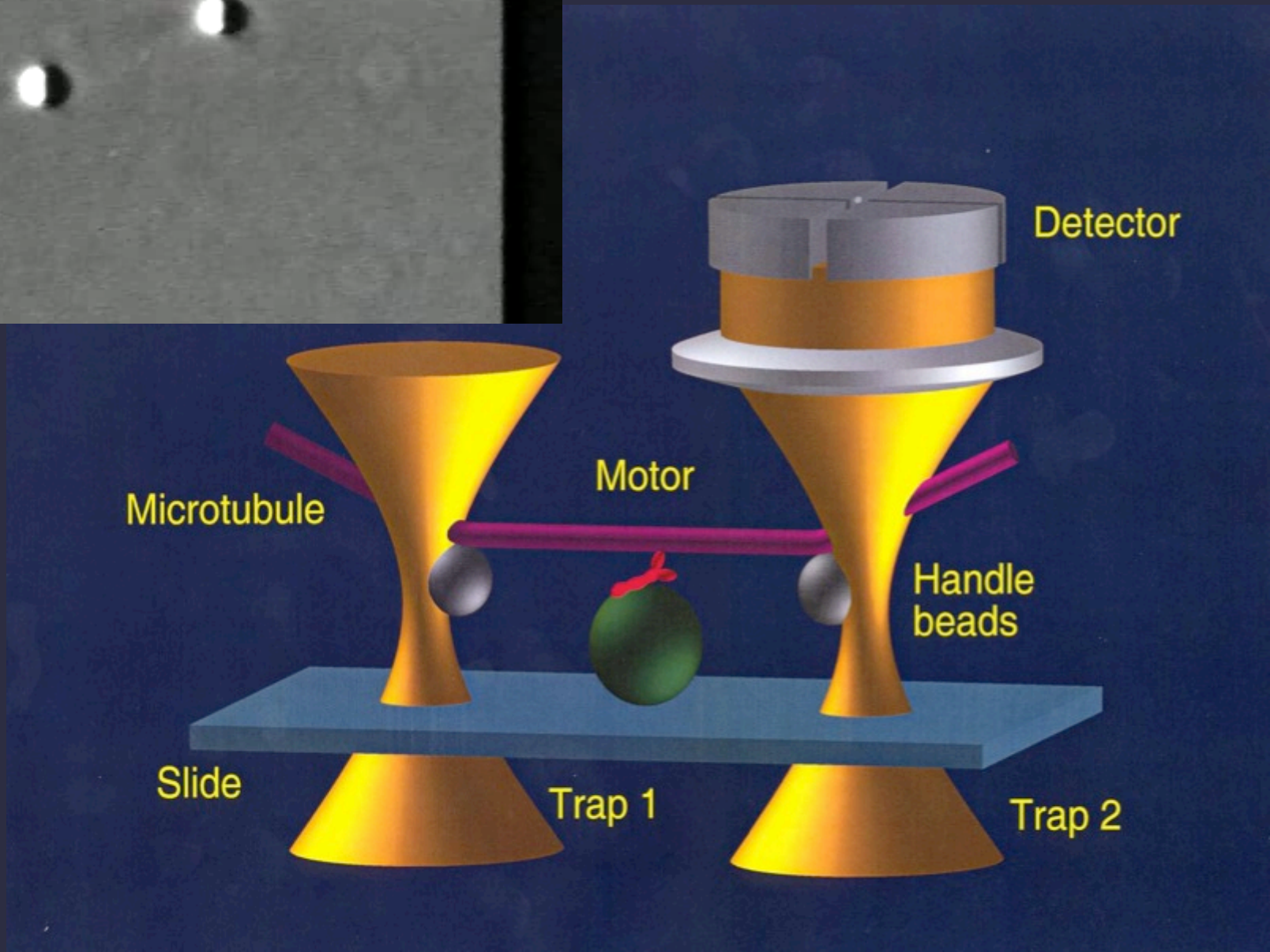

Myosin: averaged power strokes

(Veigel et al. Nature ‘99, 398, 530)

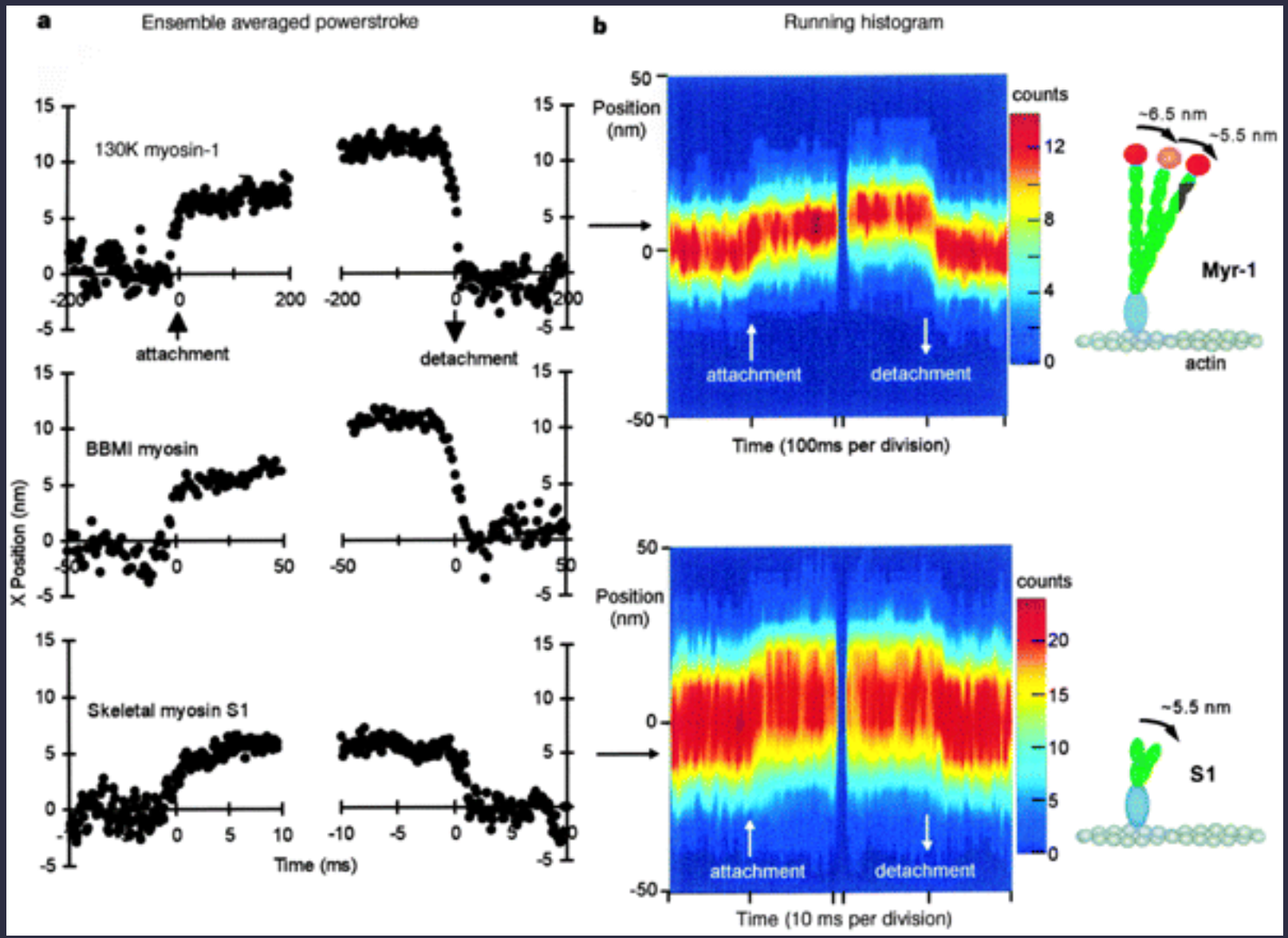

Myosin Power Stroke

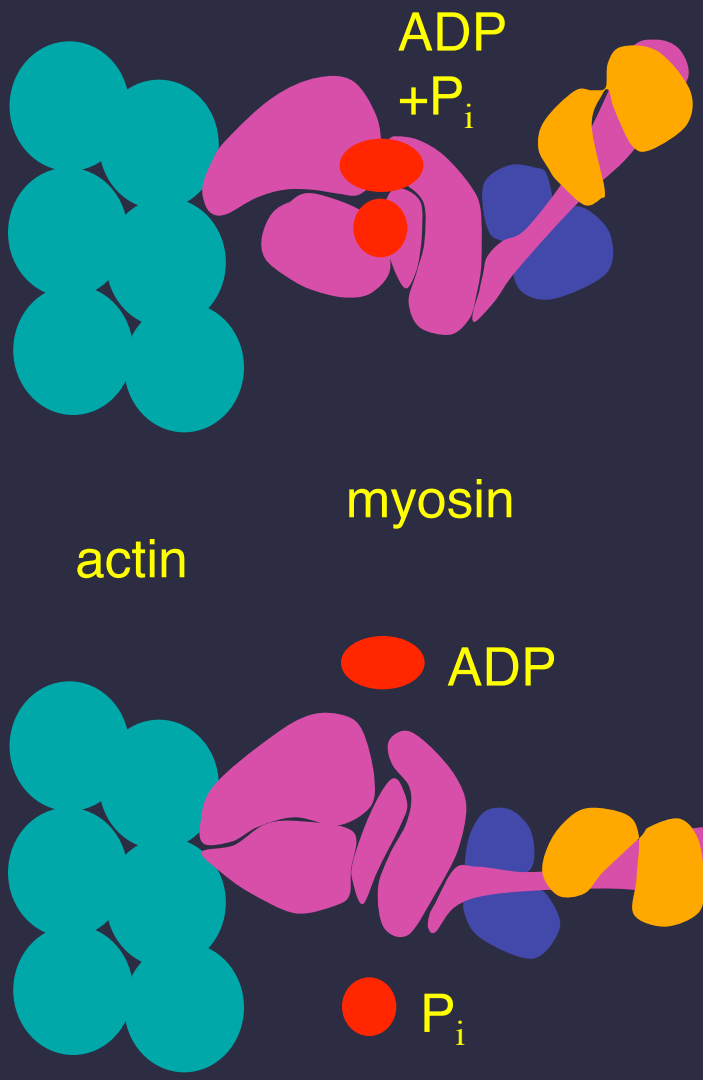

Mechano-chemical cycle:

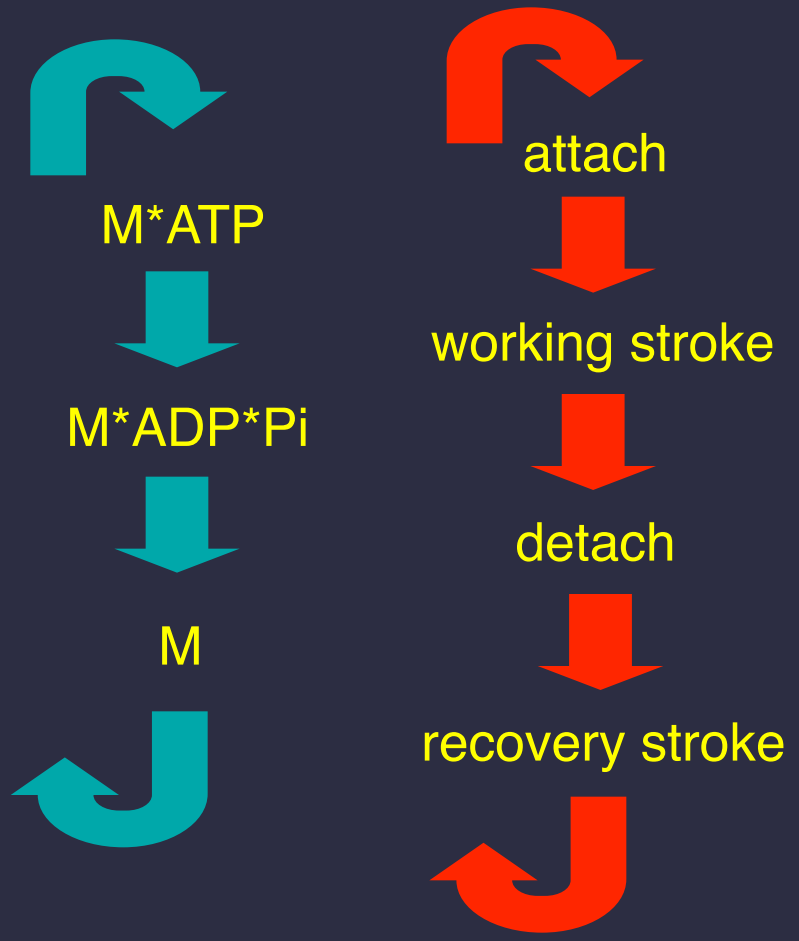

Conformational Change of Single ncd Molecule

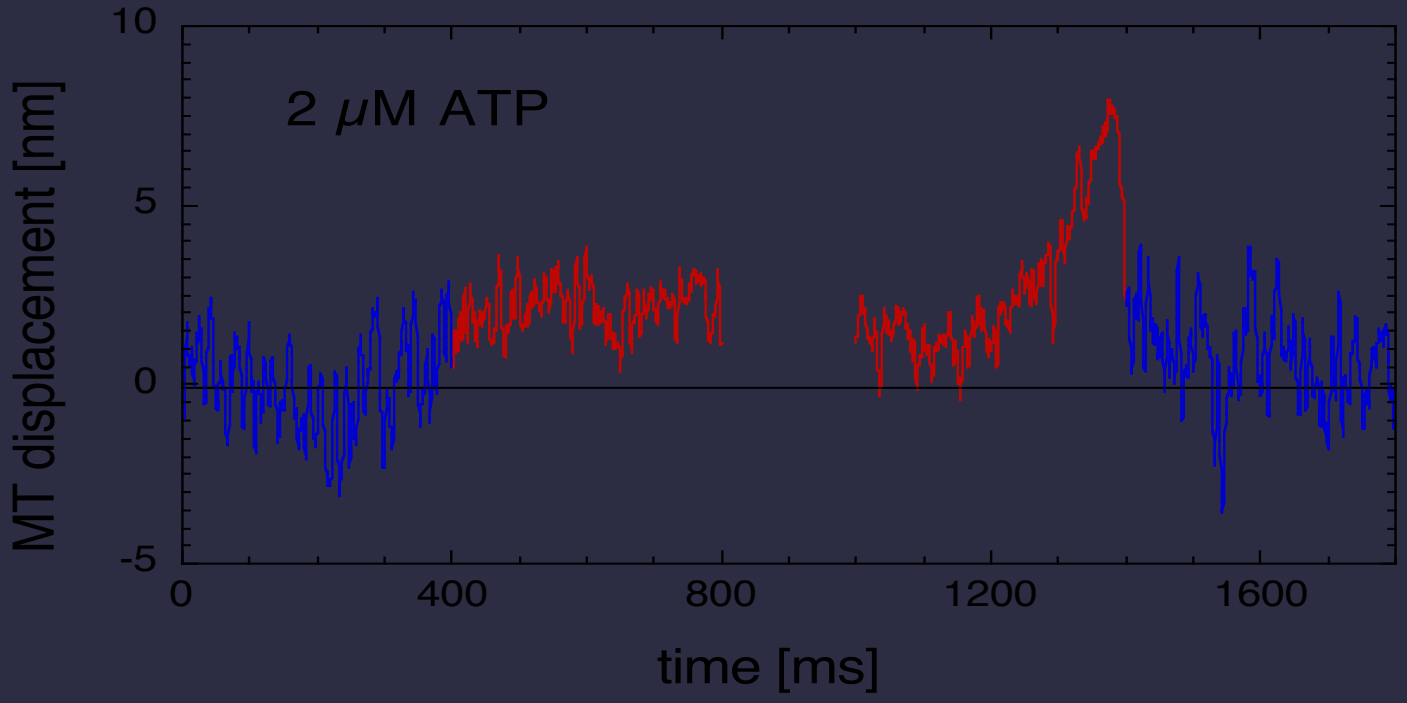

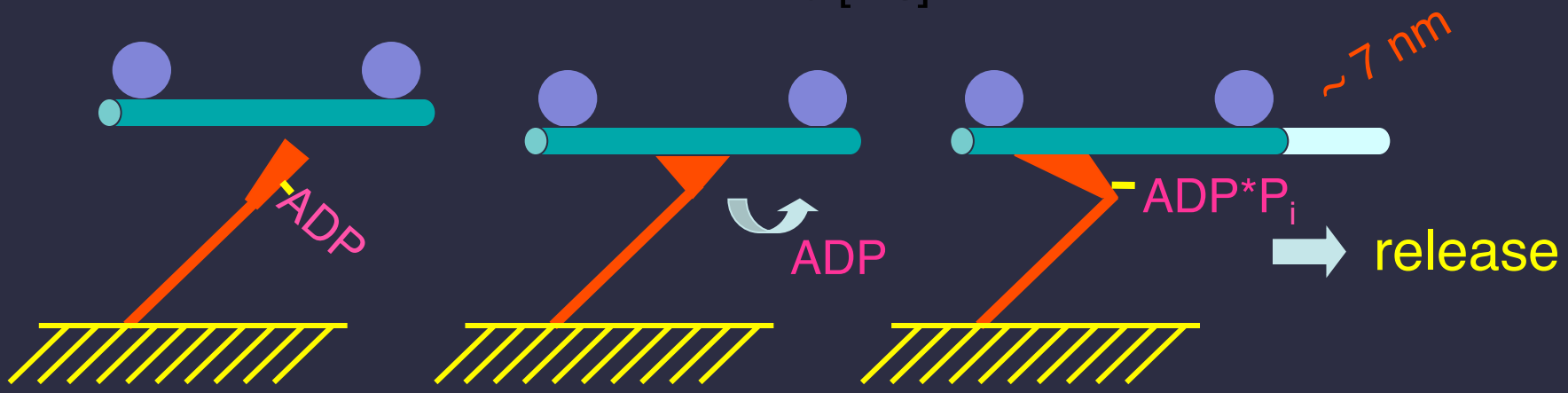

DeCastro, Fondecave, Clarke, Schmidt, Stewart, Nature Cell Biology (2000), 2:724

Single Molecule Bead Assay

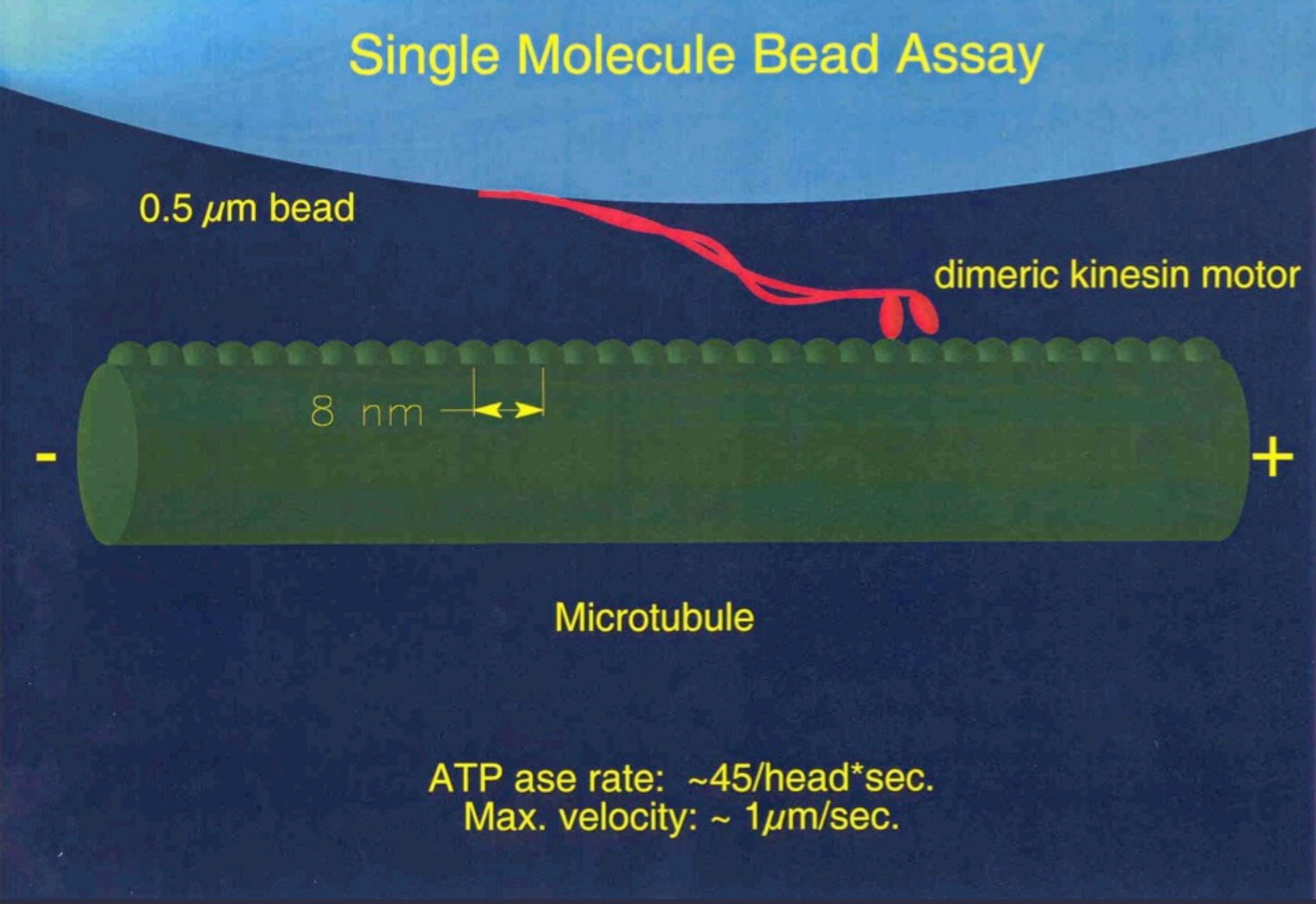

ATP ase rate: ~45/head*sec.
Max. velocity: ~ 1μm/sec.

Stepping and Stalling of a Single Kinesin Molecule

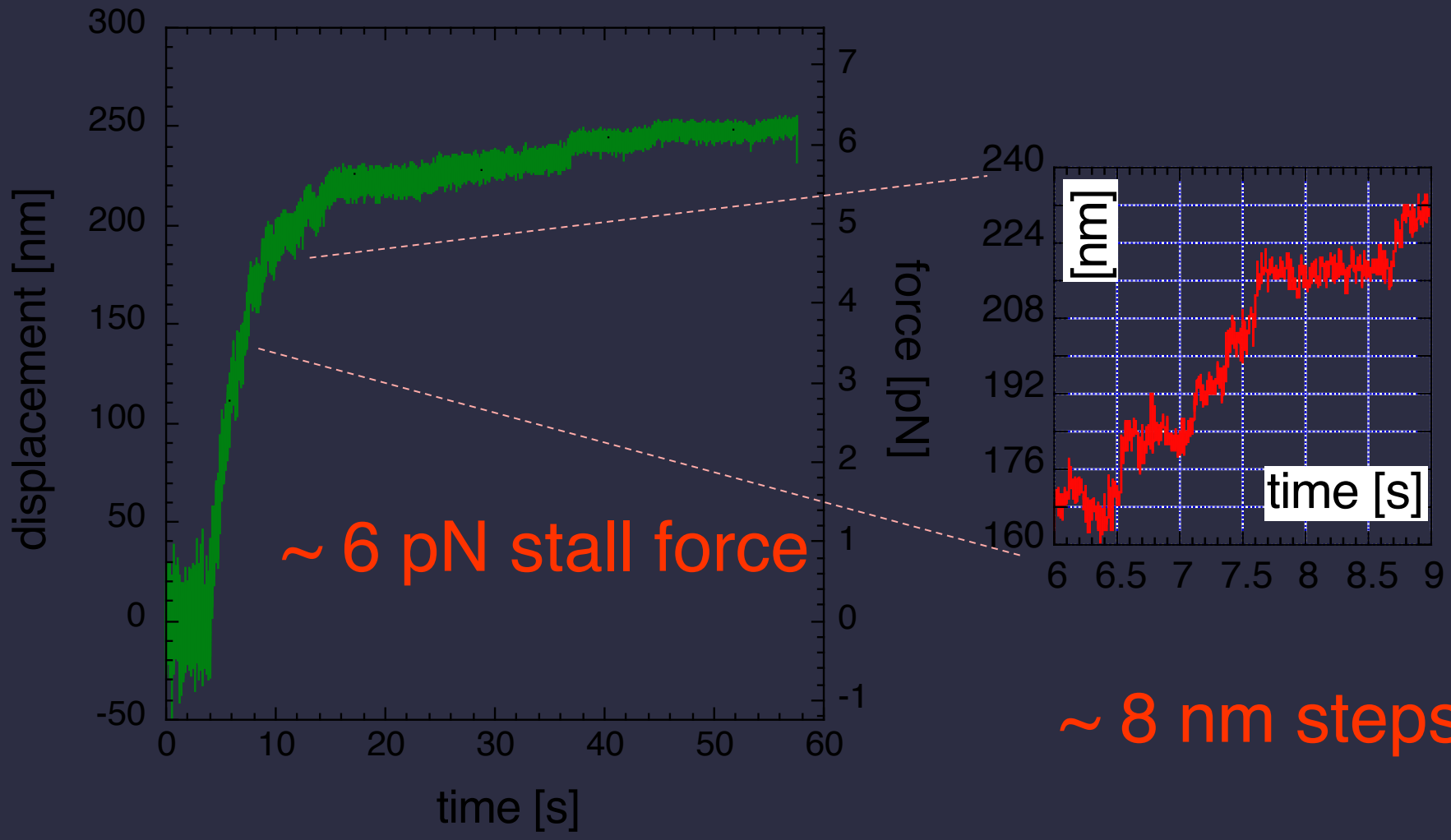

Svoboda, Schmidt, Schnapp, Block, Nature (1993), 365: 721

Randomness parameter

$$r := \lim_{t \to \infty} \frac{\langle x^2(t) \rangle - \langle x(t) \rangle^2}{d \langle x(t) \rangle}$$

Δt=const.

"clockwork"

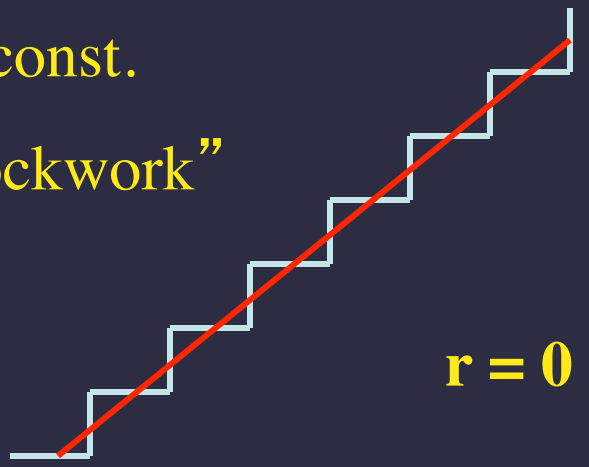

r = 0

k k k k k
1 -> 2 -> 3 -> 4 -> 5 -> 6

Δt exponentially distributed

Poisson process

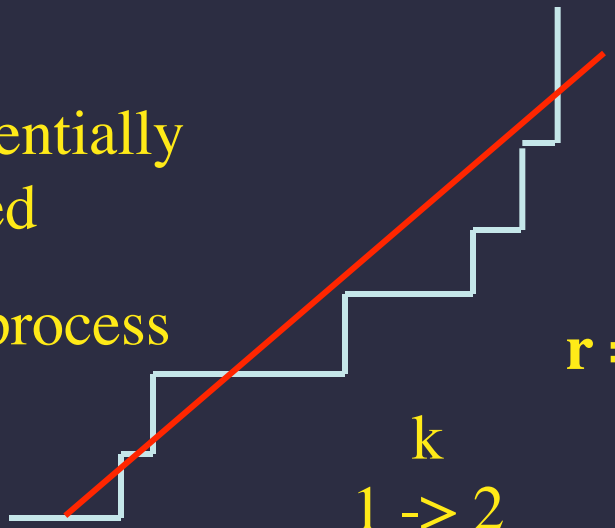

r = 1

k
1 -> 2

Randomness parameter for single kinesin

(Visscher,Schnitzer, Block (‘99), Nature 400, 184)

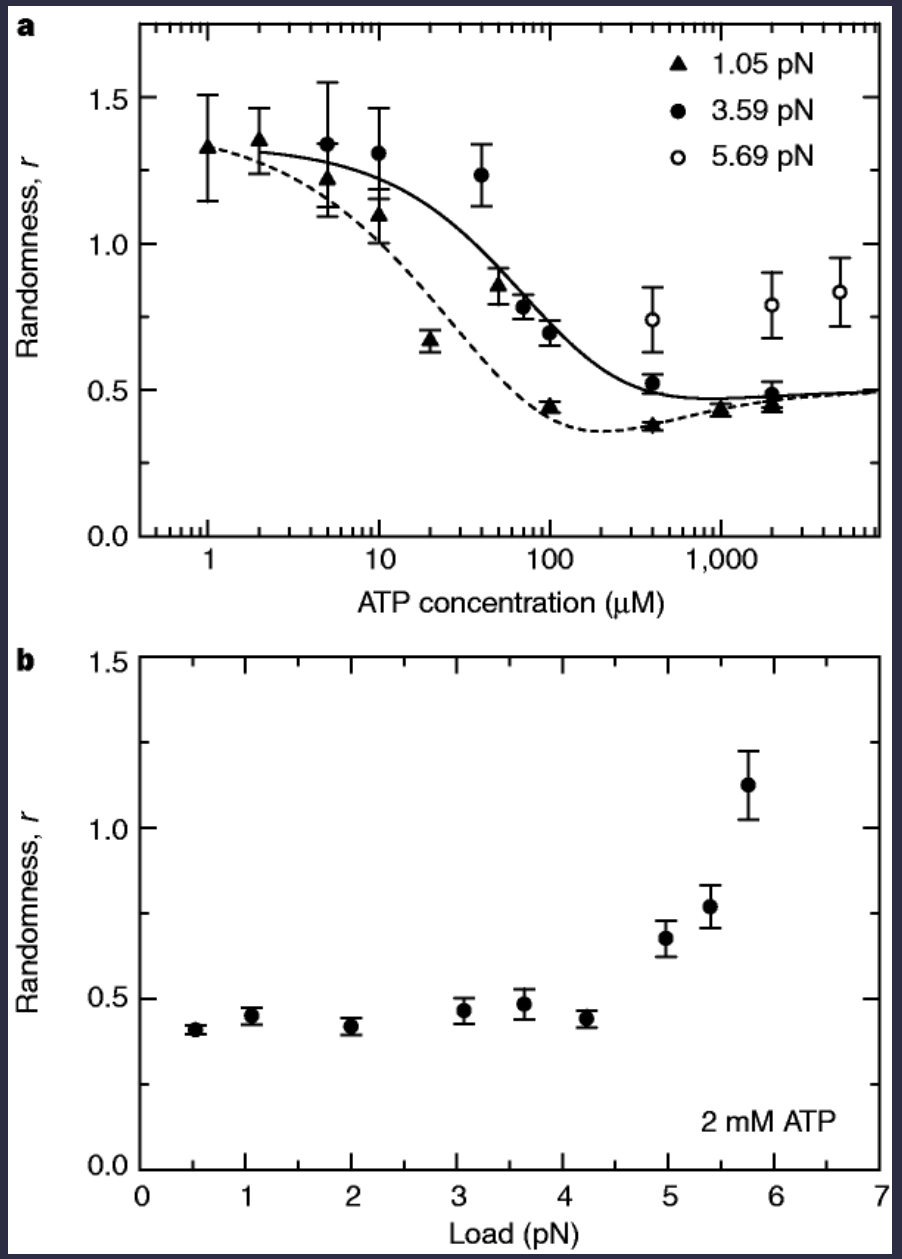

Thermal Motion of a Trapped/Tethered Particle

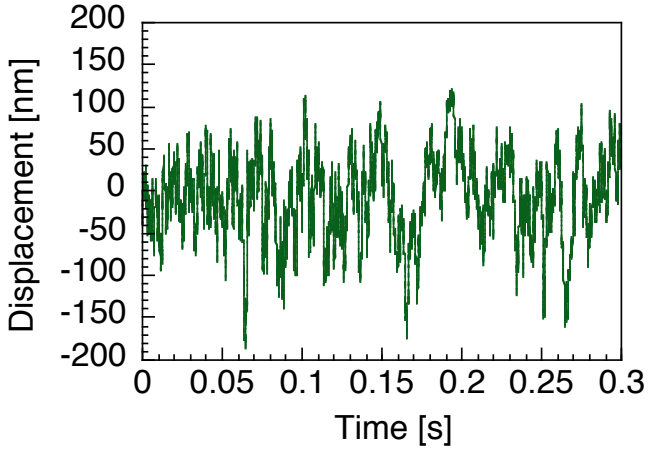

Time series:

$$\mathrm{var}(x) = \langle x^2 \rangle - \langle x \rangle^2 = \frac{k_B T}{\kappa}$$

Spectrum:

$$S(f) = \frac{k_B T}{\pi^2 \gamma (f_c^2 + f^2)}$$

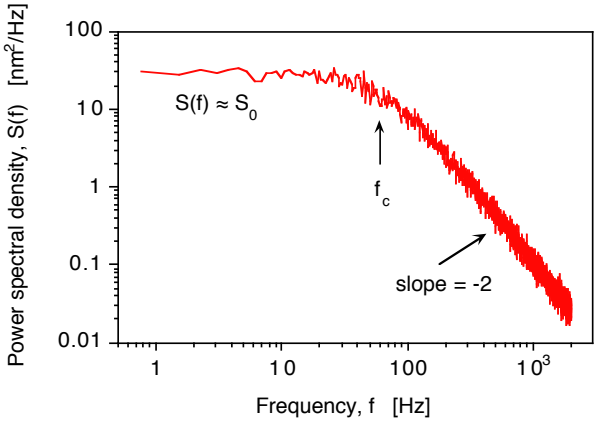

$$f_c = \frac{\kappa}{2\pi\gamma}, \qquad S_0 = \frac{4\gamma k_B T}{\kappa^2}$$

trapped bead attached to motor: $\mathrm{var}(x) = \dfrac{k_B T}{\kappa_{trap} + \kappa_{motor}}$

Efficiency, Invertability and Processivity of Molecular Motors

F. Jülicher, Institut Curie, Paris

A. Parmeggiani
L. Peliti (Naples)
A. Ajdari (Paris)
J. Prost (Paris)

http://www.curie.fr/~julicher

Mechano-chemical coupling

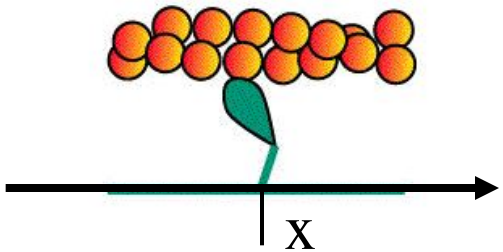

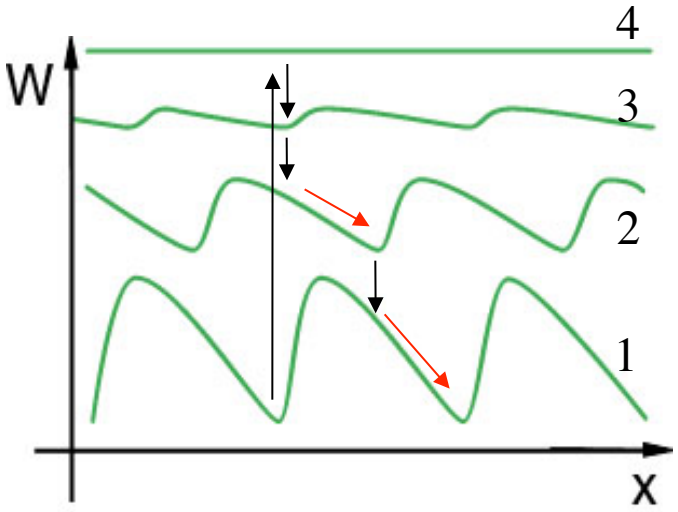

$$\partial_t P_i + \partial_x J_i = -\sum_{j\neq i} \omega_{ij} P_i + \sum_{j\neq i} \omega_{ji} P_j$$

$$J_i = -\mu(k_B T \partial_x P_i + P_i \partial_x W_i - f_{ext} P_i)$$

mean velocity

$$v = \int_0^l dx \sum_i J_i$$

Example: weakly bound state

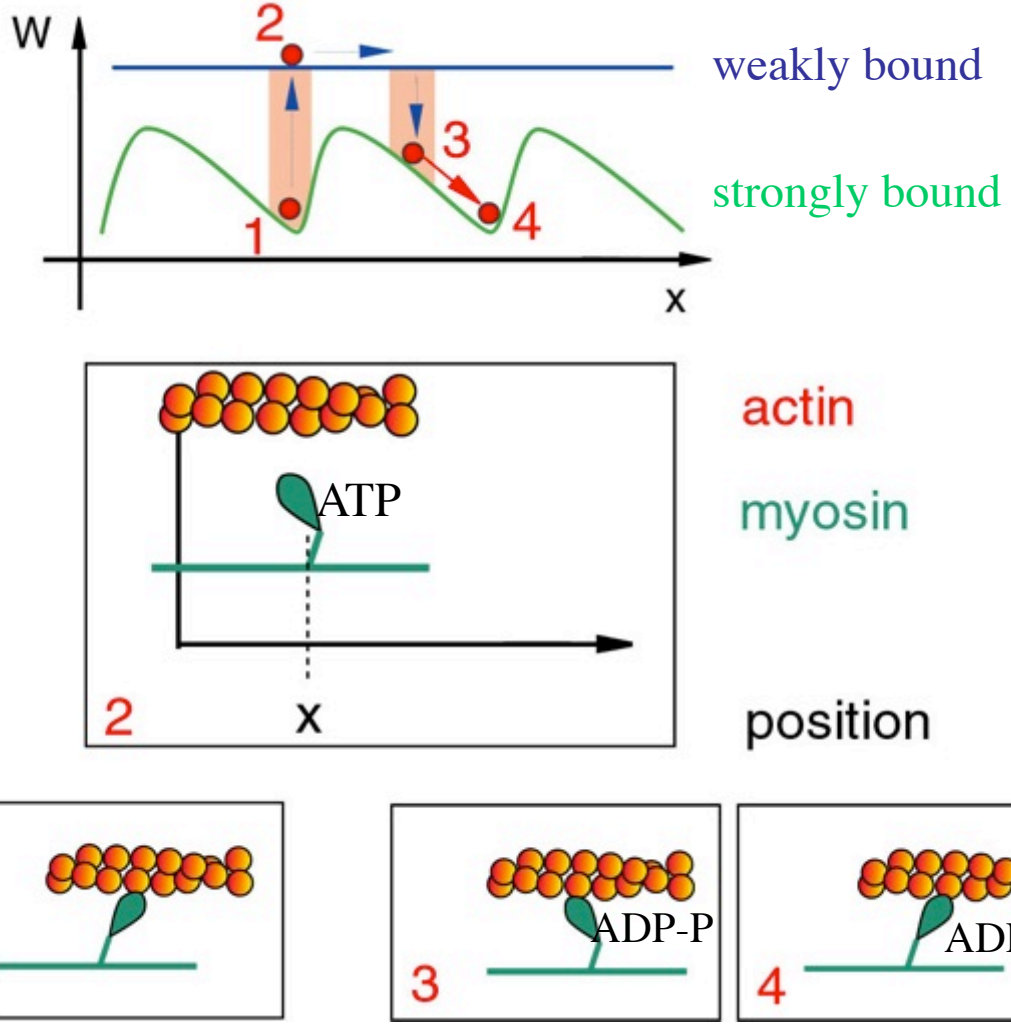

Example: identical shifted states

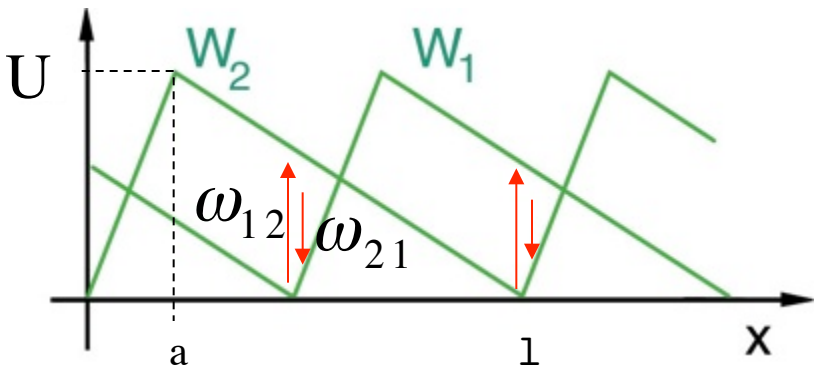

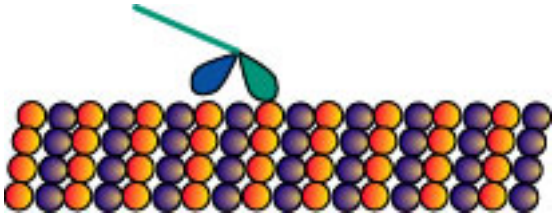

$$\omega_{12} = \omega e^{(\Delta\mu - \Delta W)/kT}$$

$$\omega_{21} = \omega$$

$$\frac{U}{k_B T} = 20 \qquad \xi = 7.4 \cdot 10^{-4} kg/s$$

$$\frac{a}{l} = 0.1 \qquad l = 16nm$$

chemical free energy of hydrolysis:

$$\Delta\mu = \mu_{ATP} - \mu_{ADP} - \mu_P$$

$$\mu_i \approx \mu_i^0 + kT \ln(C_i / C_i^0)$$

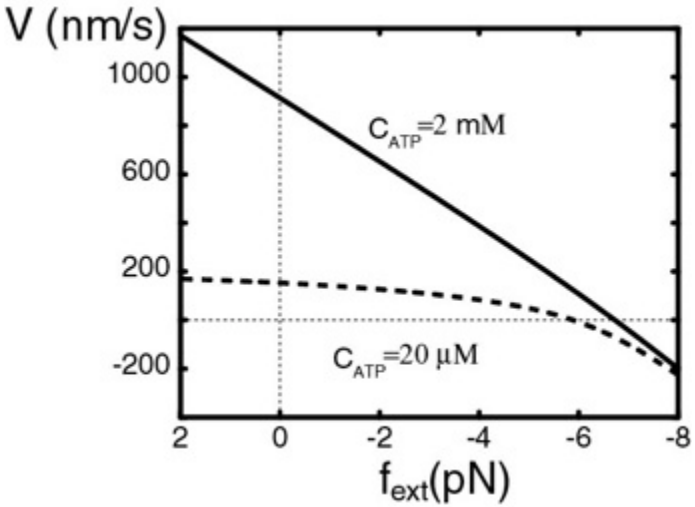

Dissipation rates

motion within a state:

$$\dot{Q}_i = \int_0^l dx\, J_i\, \partial_x H_i \geq 0$$

$$H_i = W_i - f_{ext} x + k_B T \ln(P_i)$$

chemical transitions:

$$\dot{Q}_\alpha = \int_0^l dx\, (\omega_{12} P_1 - \omega_{21} P_2)(H_1 - H_2 + \Delta\mu) \geq 0$$

total internal dissipation of the motor:

$$\dot{Q} = \dot{Q}_1 + \dot{Q}_2 + \dot{Q}_\alpha \geq 0$$

Efficiency of energy transduction

Energy conservation:

$$\dot{Q} = r\Delta\mu + f_{ext}v$$

mechanical work

chemical work

total internal dissipation

f_{ext} force

v velocity

$\Delta\mu$ chemical energy

r chemical rate

$$\eta = -\frac{f_{ext}v}{r\Delta\mu}$$

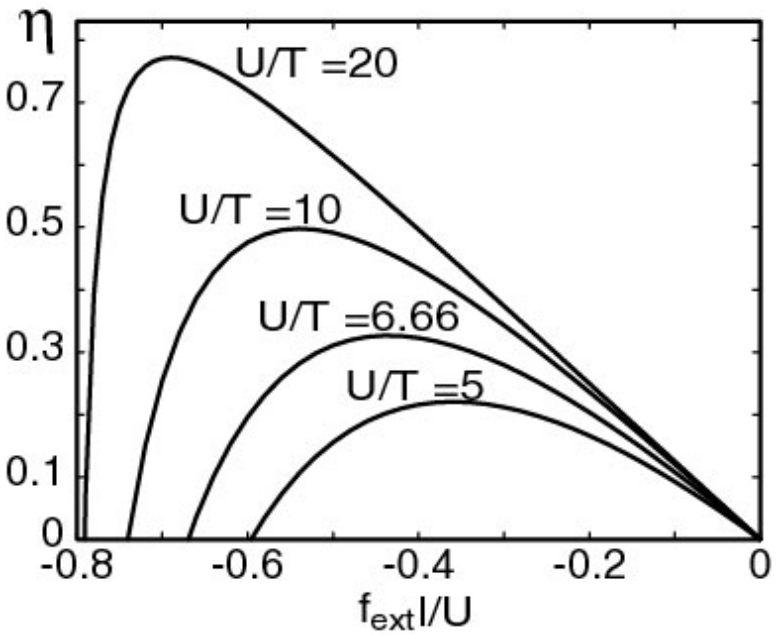

A. Parmeggiani, F. Jülicher, A. Ajdari and J. Prost, PRE 60, 2127 (1999)

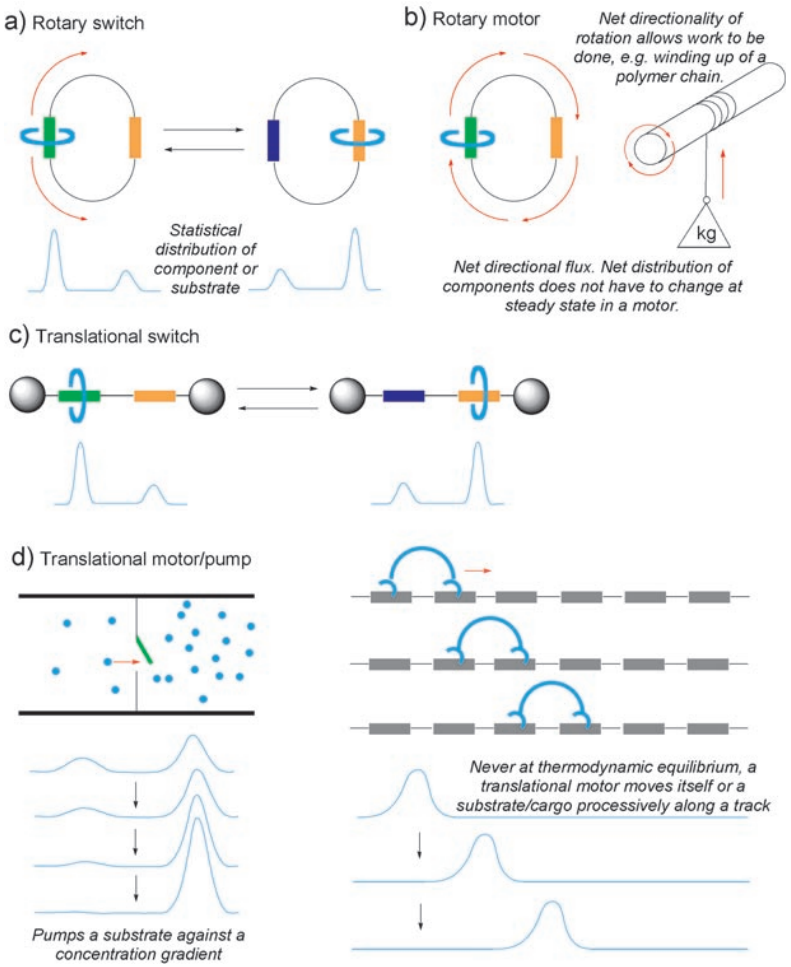

Figure 1. The fundamental difference between a "switch" and a "motor" at the molecular level. Both translational and rotary switches influence a system as a function of the switch state. They switch between two or more, often equilibrium, states. Motors, however, influence a system as a function of the trajectory of their components or a substrate. Motors function repetitively and progressively on a system; the affect of a switch is undone by resetting the machine. a) Rotary switch. b) Rotary motor. c) Translational switch. d) Translational motor or pump.

Carter, N. J., & Cross, R. A. (2005). Mechanics of the kinesin step. *Nature*, *435*(7040), 308–312.

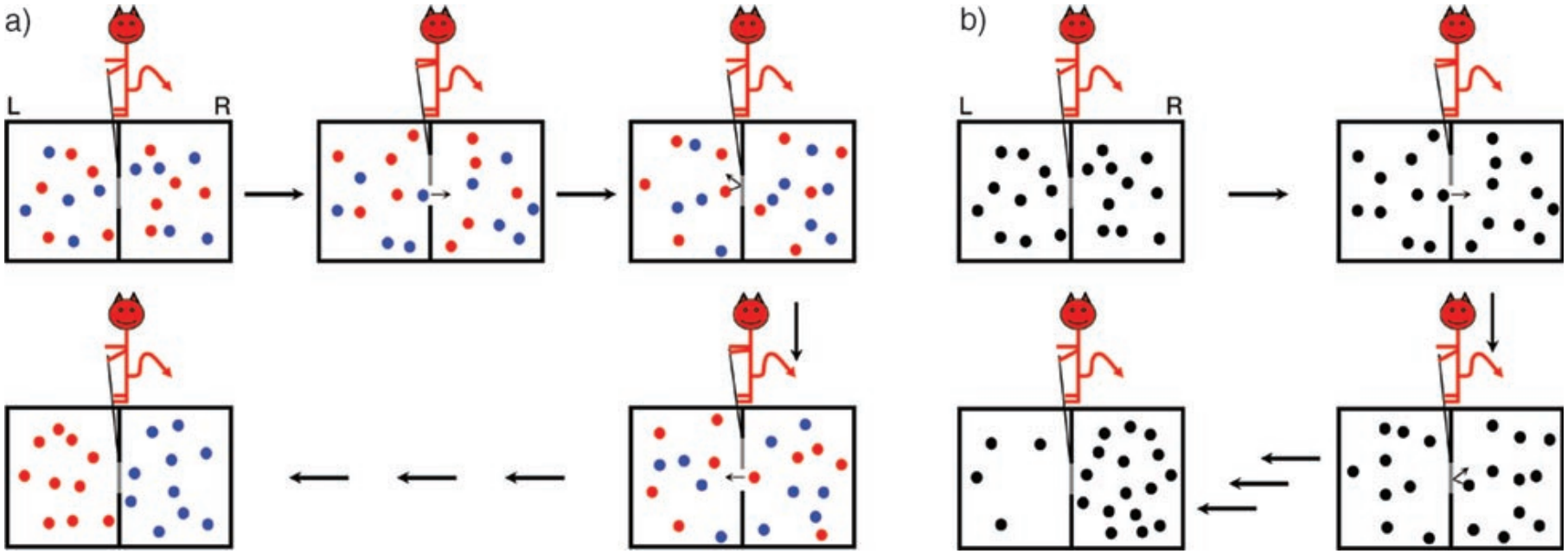

Figure 2. a) Maxwell's "temperature demon" in which a gas at uniform temperature is sorted into "hot" and "cold" molecules.[15] Particles with energy higher than the average are represented by red dots while blue dots represent particles with energies lower than the average. All mechanical operations carried out by the demon involve no work—that is, the door is frictionless and it is opened and closed infinitely slowly. The depiction of the demon outside the vessel is arbitrary and was not explicitly specified by Maxwell. b) A Maxwellian "pressure demon" in which a pressure gradient is established by the door being opened only when a particle in the left compartment approaches it.[15c]

Carter, N. J., & Cross, R. A. (2005). Mechanics of the kinesin step. *Nature*, *435*(7040), 308–312.

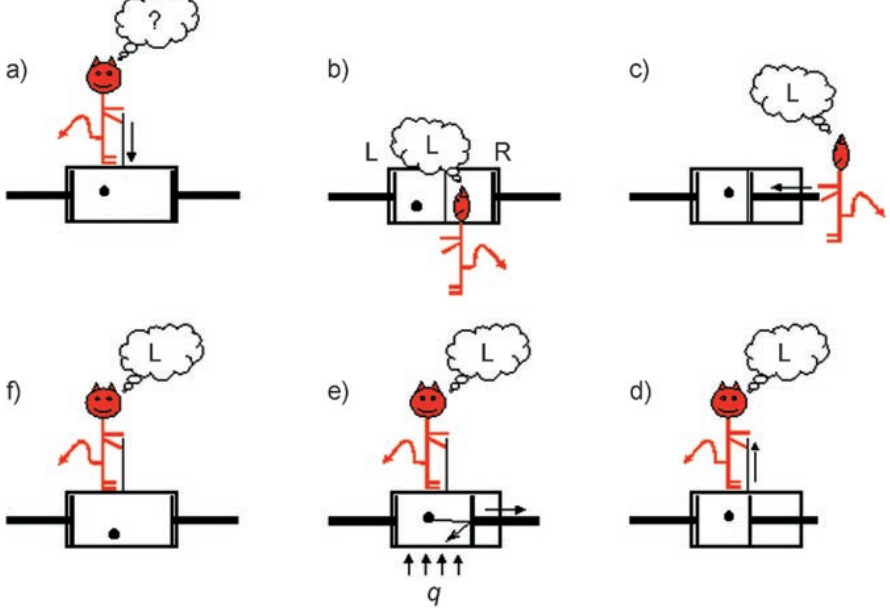

Figure 3. Szilard's engine which utilizes a "pressure demon".[17] a) Initially a single Brownian particle occupies a cylinder with a piston at either end. A frictionless partition is put in place to divide the container into two compartments (a→b). b) The demon then detects the particle and determines in which compartment it resides. c) Using this information, the demon is able to move the opposite piston into position without meeting any resistance from the particle. d) The partition is removed, allowing the "gas" to expand against the piston, doing work against any attached load (e). To replenish the energy used by the piston and maintain a constant temperature, heat must flow into the system. To complete the thermodynamic cycle and reset the machine, the demon's memory of where the particle was must be erased (f→a). To fully justify the application of a thermodynamic concept such as entropy to a single-particle model, a population of Szilard devices is required. The average for the ensemble over each of these devices can then be considered to represent the state of the system, which is comparable to the time average of a single multi-particle system at equilibrium, in a fashion similar to the statistical mechanics derivation of thermodynamic quantities.

Carter, N. J., & Cross, R. A. (2005). Mechanics of the kinesin step. *Nature*, *435*(7040), 308–312.

Figure 4. a) Smoluchowski's trapdoor: an "automatic" pressure demon (the directionally discriminating behavior is carried out by a wholly mechanical device, a trapdoor which is intended to open when hit from one direction but not the other).[16] Like the pressure demon shown in Figure 2b, Smoluchowski's trapdoor aims to transport particles selectively from the left compartment to the right. However, in the absence of a mechanism whereby the trapdoor can dissipate energy it will be at thermal equilibrium with its surroundings. This means it must spend much of its time open, unable to influence the transport of particles. Rarely, it will be closed when a particle approaches from the right and will open on collision with a particle coming from the left, thus doing its job as intended. Such events are balanced, however, by the door snapping shut on a particle from the right, pushing it into the left chamber. Overall, the probability of a particle moving from left to right is equal to that for moving right to left and so the trapdoor cannot accomplish its intended function adiabatically. b) Feynman's ratchet and pawl.[18] It might appear that Brownian motion of the gas molecules on the paddle wheel in the right-hand compartment can do work by exploiting the asymmetry of the teeth on the cog of the ratchet in the left-hand compartment. While the spring holds the pawl between the teeth of the cog, it does indeed turn selectively in the desired direction. However, when the pawl is disengaged, the cog wheel need only randomly rotate a tiny amount in the other direction to move back one tooth whereas it must rotate randomly a long way to move to the next tooth forward. If the paddle wheel and ratchet are at the same temperature (that is, $T_1 = T_2$) these rates cancel out. However, if $T_1 \neq T_2$ then the system will directionally rotate, driven solely by the Brownian motion of the gas molecules. Part (b) reprinted with permission from Ref. [18].

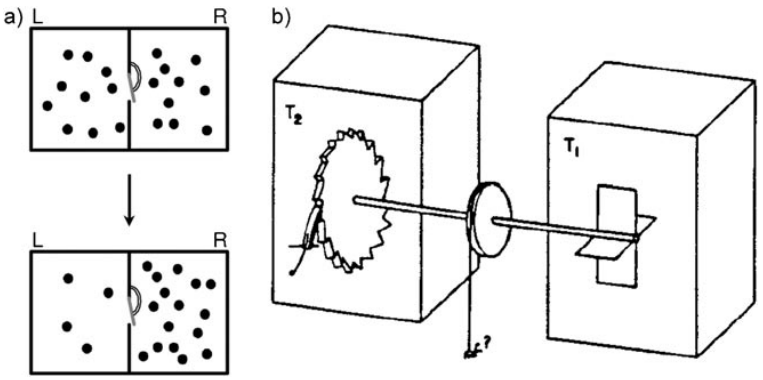

Carter, N. J., & Cross, R. A. (2005). Mechanics of the kinesin step. *Nature*, *435*(7040), 308–312.

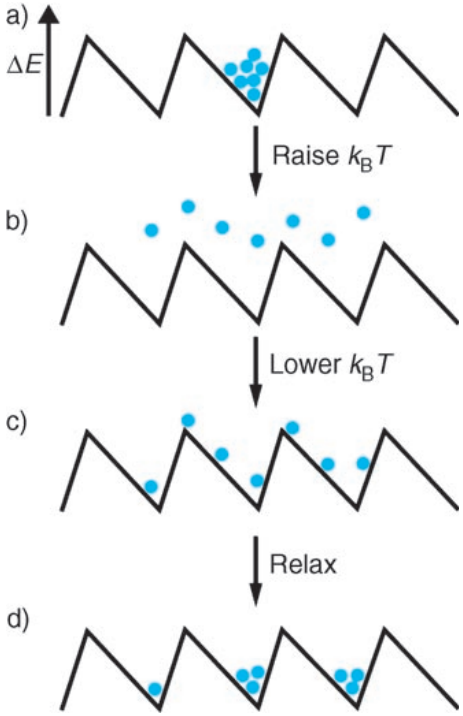

Figure 8. A temperature (or diffusion) ratchet.[39f] a) The Brownian particles start out in energy minima on the potential-energy surface with the energy barriers $\gg k_B T_1$. b) The temperature is increased so that the height of the barriers is $\ll k_B T_2$ and effectively free diffusion is allowed to occur for a short time period (much less than required to reach global equilibrium). c) The temperature is lowered to T_1 once more, and the asymmetry of the potential means that each particle is statistically more likely to be captured by the adjacent well to the right rather than the well to the left. d) Relaxation to the local energy minimum (during which heat is emitted) leads to the average position of the particles moving to the right. Repeating steps (b)–(d), progressively moves the Brownian particles further and further to the right. Note the similarities between this mechanism and that of the on–off ratchet shown in Figure 6.

Carter, N. J., & Cross, R. A. (2005). Mechanics of the kinesin step. *Nature*, *435*(7040), 308–312.

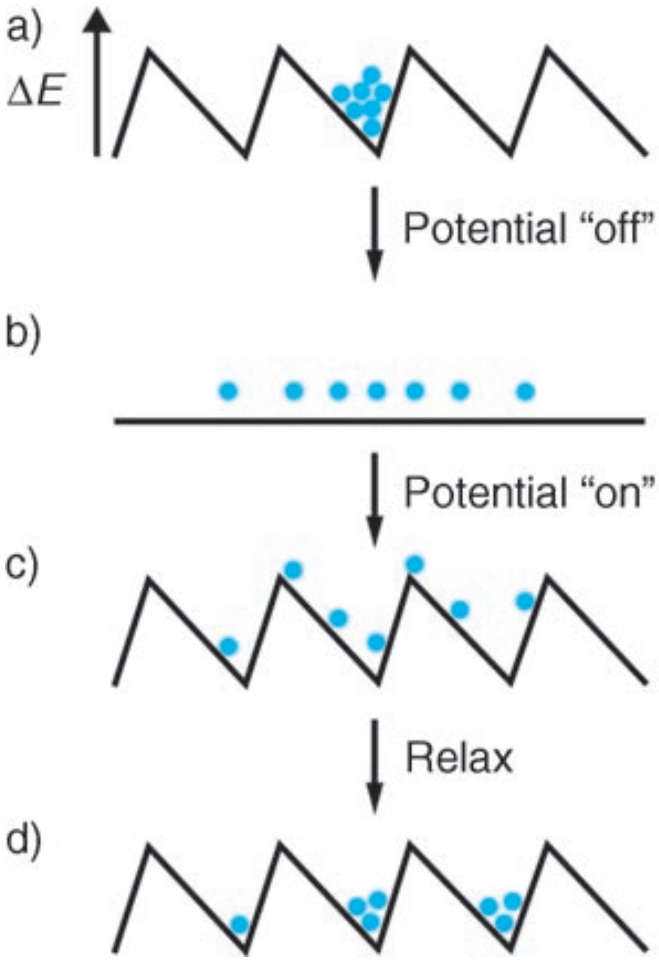

Figure 6. An example of a pulsating ratchet mechanism—an on–off ratchet.[39f] a) The Brownian particles start out in energy minima on the potential-energy surface with the energy barriers $\gg k_B T$. b) The potential is turned off so that free Brownian motion powered diffusion is allowed to occur for a short time period (much less than required to reach global equilibrium). c) On turning the potential back on again, the asymmetry of the potential means that the particles have a greater probability of being trapped in the adjacent well to the right rather than the adjacent well to the left. Note this step involves raising the energy of the particles. d) Relaxation to the local energy minima (during which heat is emitted) leads to the average position of the particles moving to the right. Repeating steps (b)–(d) progressively moves the Brownian particles further and further to the right.

Carter, N. J., & Cross, R. A. (2005). Mechanics of the kinesin step. *Nature*, *435*(7040), 308–312.

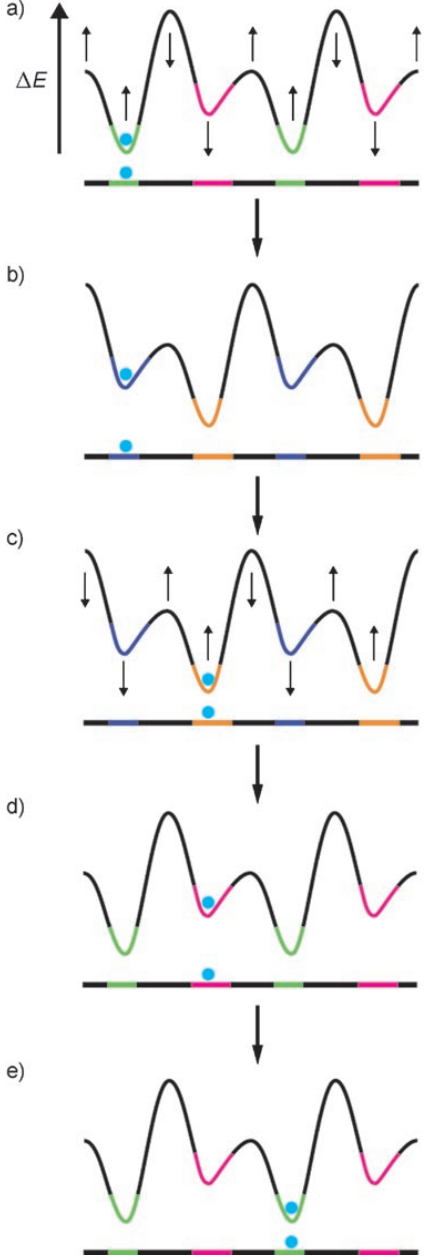

Figure 7. Another example of a pulsating ratchet mechanism—a flashing ratchet.[42b] For details of its operation, see the text.

Carter, N. J., & Cross, R. A. (2005). Mechanics of the kinesin step. *Nature*, *435*(7040), 308–312.

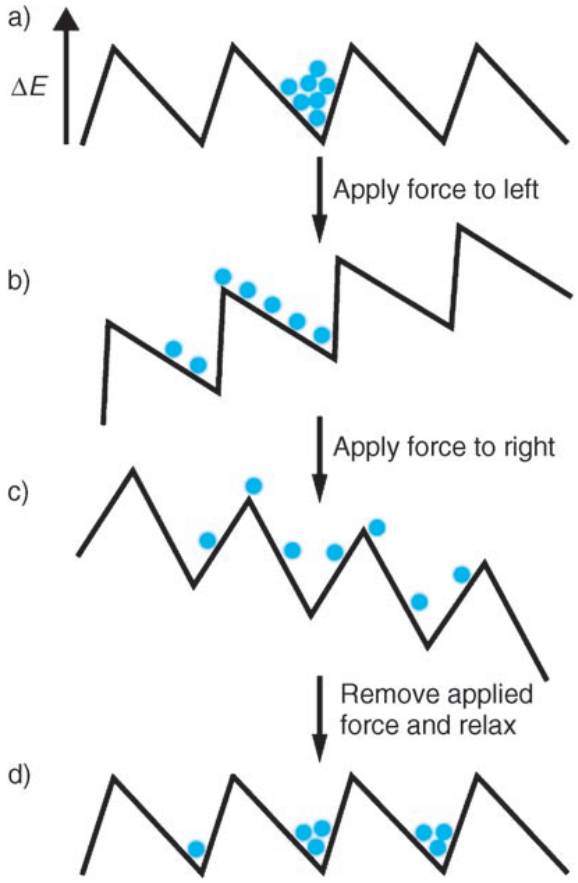

Figure 9. A rocking ratchet.[39f] a) The Brownian particles start out in energy minima on the potential-energy surface with the energy barriers $\gg k_B T$. b) A directional force is applied to the left. c) An equal and opposite directional force is applied to the right. d) Removal of the force and relaxation to the local energy minimum leads to the average position of the particles moving to the right. Repeating steps (b)–(d) progressively moves the Brownian particles further and further to the right.

Carter, N. J., & Cross, R. A. (2005). Mechanics of the kinesin step. *Nature*, *435*(7040), 308–312.

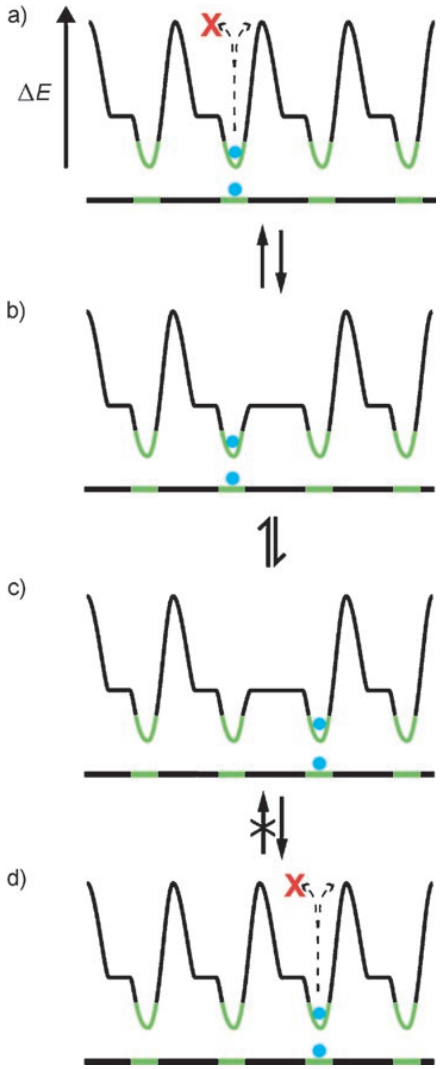

Figure 10. A type of information ratchet mechanism for transport of a Brownian particle along a potential-energy surface.[39h, 42b, 45] Dotted arrows indicate the transfer of information that signals the position of the particle. If the signal is distance-dependent—say, energy transfer from an excited state which causes lowering of an energy barrier—then the asymmetry in the particle's position between two barriers provides the "information" which transports the particle directionally along the potential energy surface.

Carter, N. J., & Cross, R. A. (2005). Mechanics of the kinesin step. *Nature*, *435*(7040), 308–312.

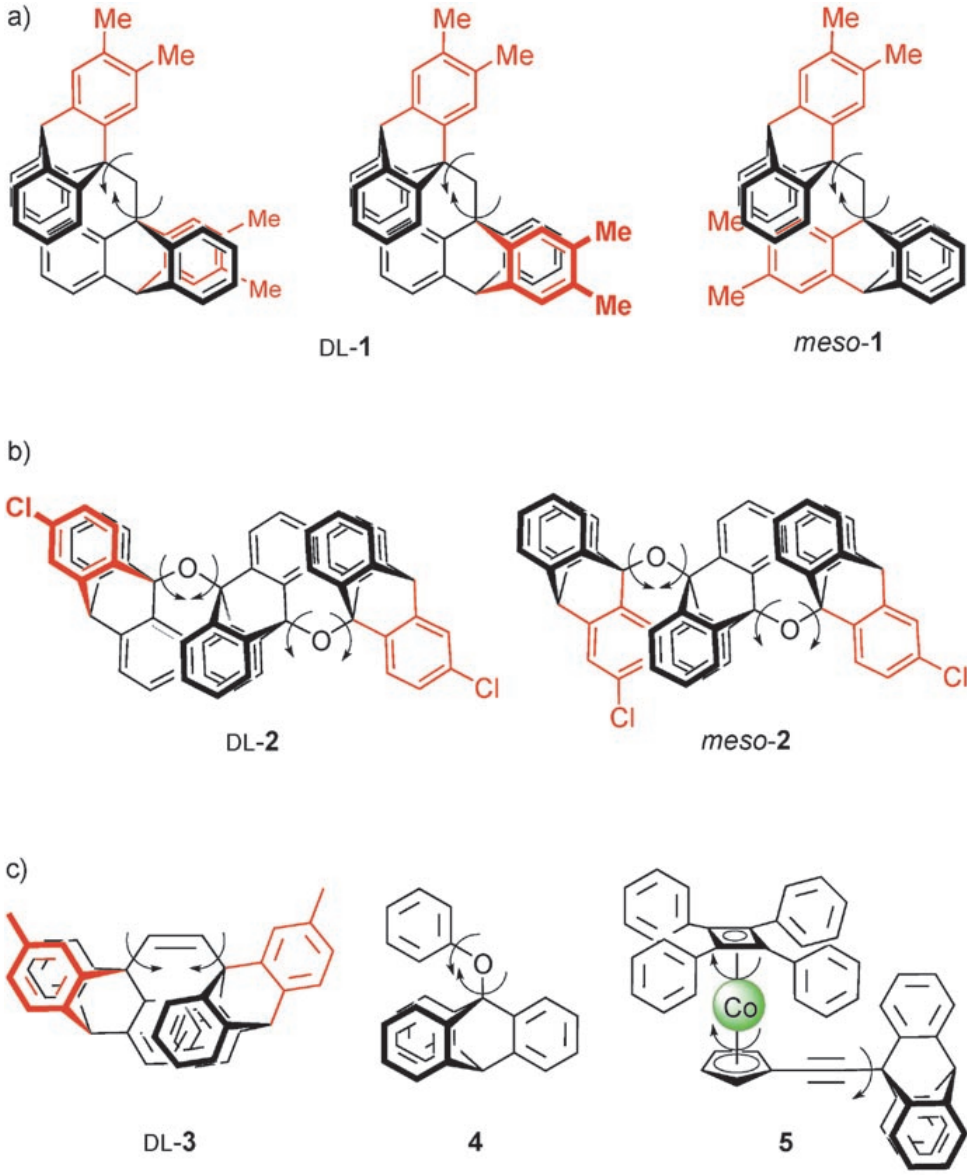

Scheme 1. a) The three residual diastereoisomers of molecular gear **1**.[57b] Correlated disrotation maintains the phase relationship between the labeled blades (shown here in red) for each isomer. Interconversion between isomers ("gear slippage") requires correlated conrotation or uncorrelated rotation. b) Molecular gear train **2**.[60] c) Vinyl molecular gear **3** (shown as the racemic residual diastereomer);[61] a molecular gear **4** with a 2:3 gearing ratio;[62j] and a molecular gear **5** based on revolution around a metallocene and with a 3:4 gearing ratio.[63] The arrows show correlated motions but are not meant to imply intrinsic directionality.

Carter, N. J., & Cross, R. A. (2005). Mechanics of the kinesin step. *Nature*, *435*(7040), 308–312.

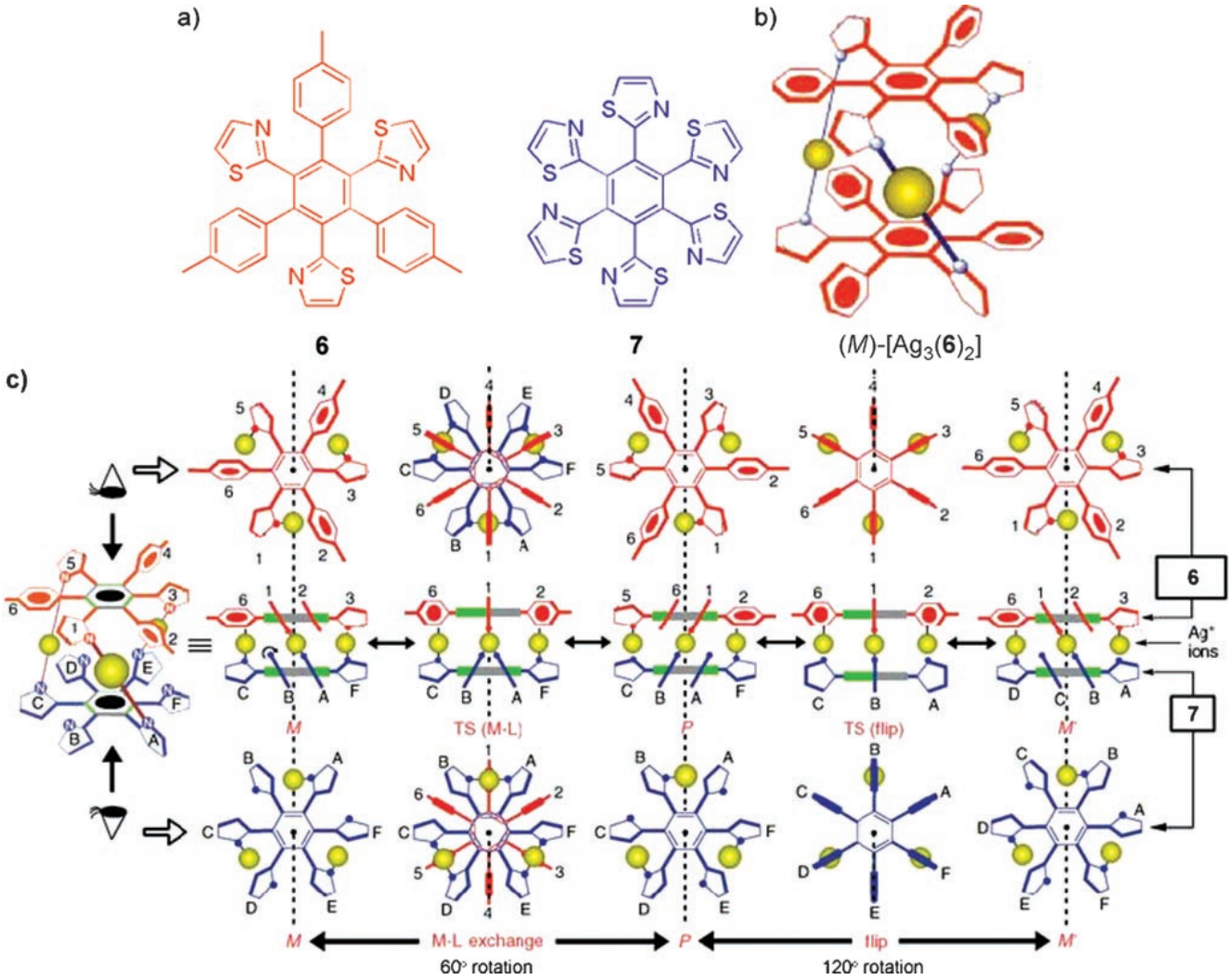

Figure 11. a) Chemical structure of tris-monodentate disk-shaped ligand **6** and hexakis-monodentate ligand **7**.[65] b) Schematic representation of complex $[Ag_3(\mathbf{6})_2]$ arbitrarily shown as its *M*-helical enantiomer. c) Description of the two correlated rotation processes occurring in $[Ag_3(\mathbf{6})(\mathbf{7})]$. The direction of rotation for an $M \rightarrow P$ transition through ligand exchange is opposite to that for the potentially subsequent $P \rightarrow M'$ transition by the nondissociative flip mechanism. Schematic representations reprinted with permission from Refs. [65a,c].

Carter, N. J., & Cross, R. A. (2005). Mechanics of the kinesin step. *Nature*, *435*(7040), 308–312.

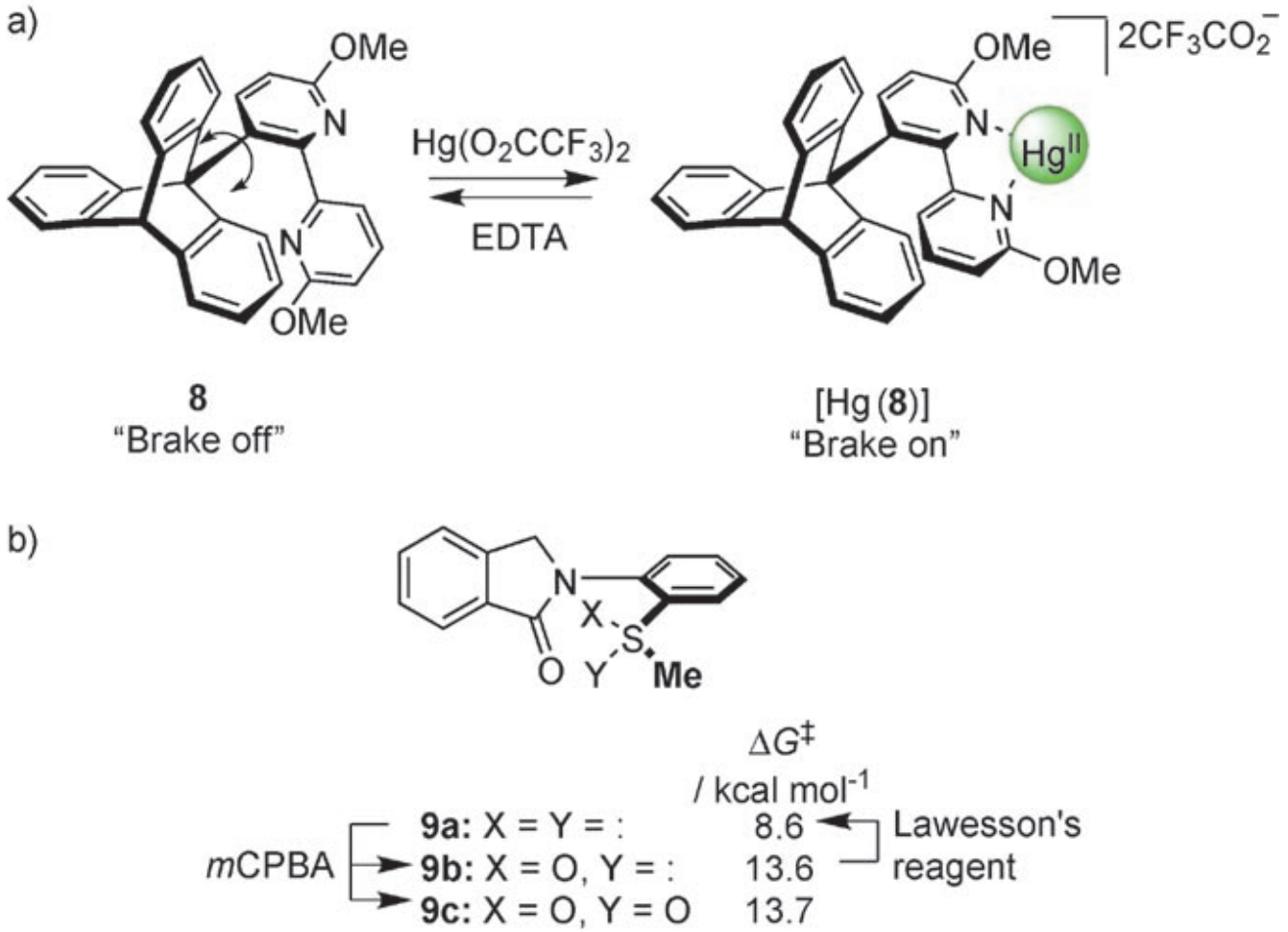

Scheme 2. "Molecular brakes" induced by a) metal-ion binding[68] and b) redox chemistry.[70] EDTA = ethylenediaminetetraacetate, *m*CPBA = *meta*-chloroperbenzoic acid.

Carter, N. J., & Cross, R. A. (2005). Mechanics of the kinesin step. *Nature*, *435*(7040), 308–312.

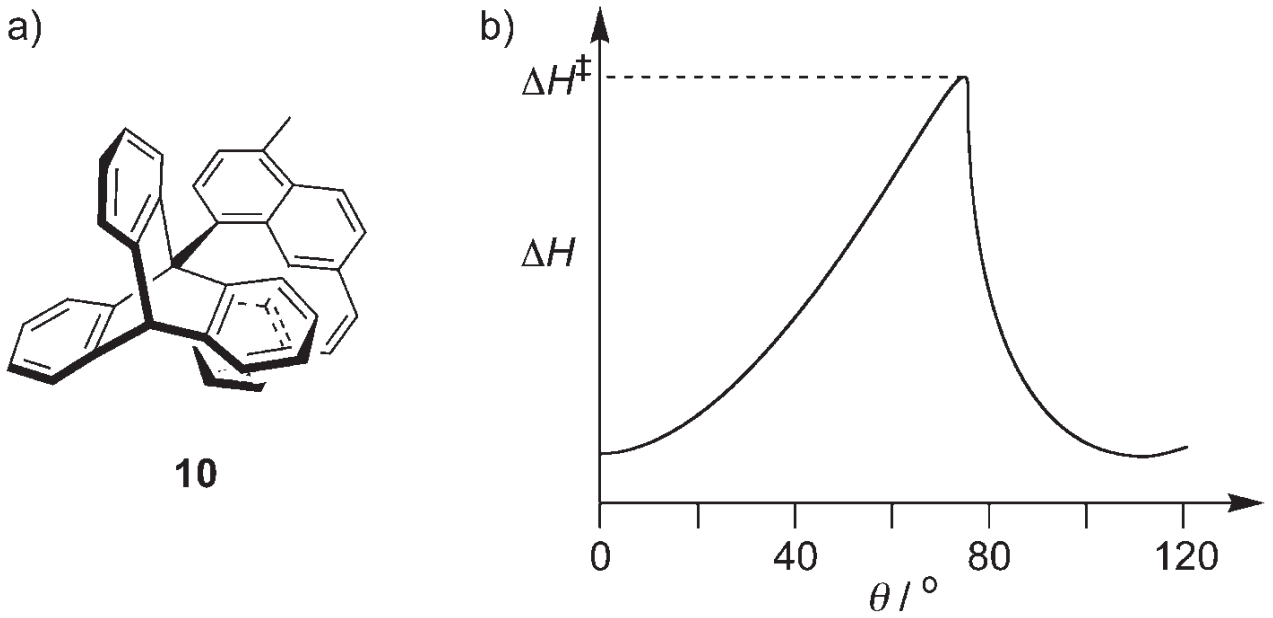

Figure 12. a) Kelly's molecular realization (**10**) of Feynman's adiabatic ratchet and pawl which does not rotate directionally at equilibrium.[72] b) Schematic representation of the calculated enthalpy changes for rotation around the single degree of internal rotational freedom in **10**.

Carter, N. J., & Cross, R. A. (2005). Mechanics of the kinesin step. *Nature*, *435*(7040), 308–312.

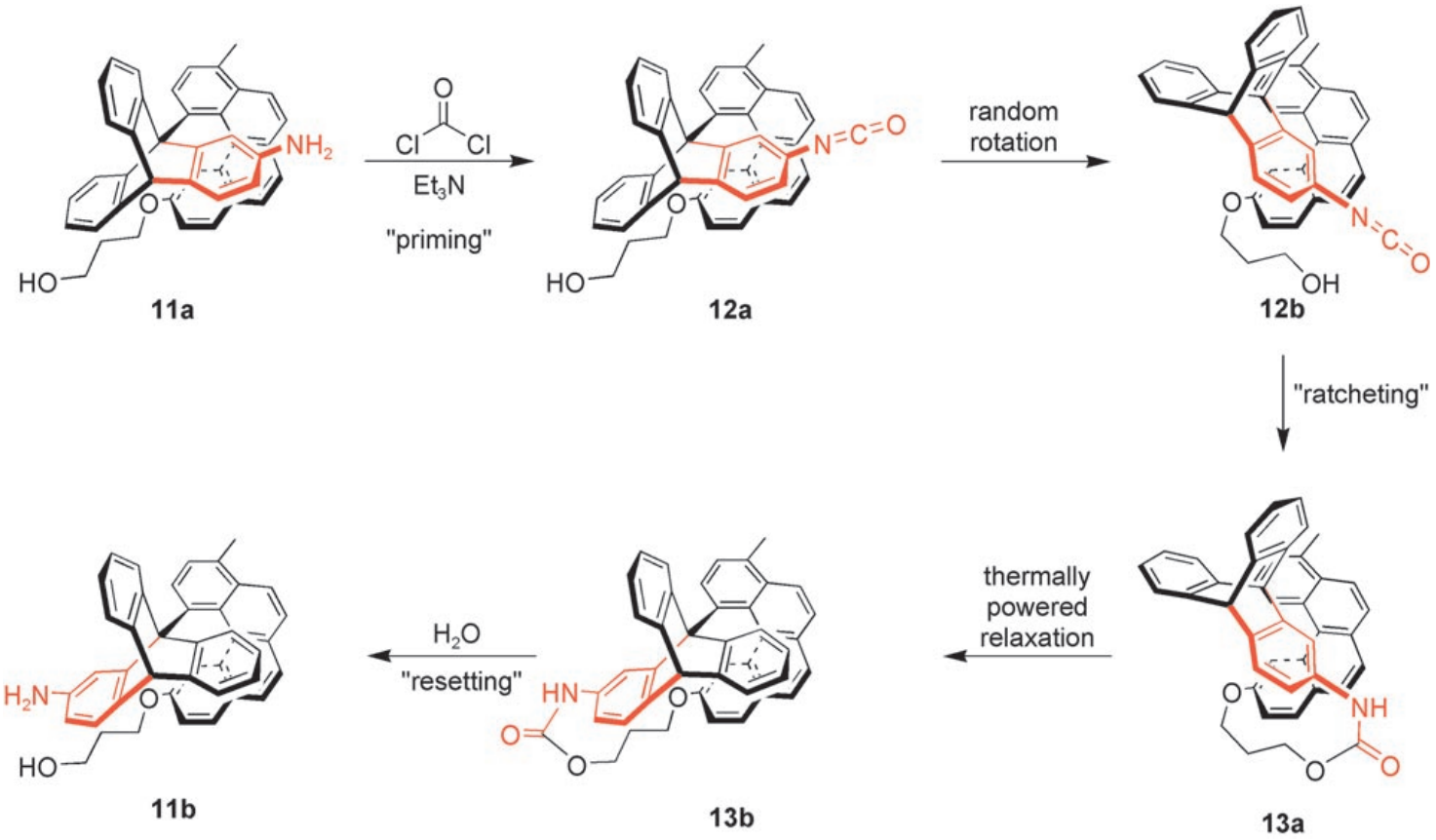

Scheme 3. A chemically powered unidirectional rotor.[76] Priming of the rotor in its initial state with phosgene (**11a**→**12a**) allows a chemical reaction to take place when the helicene rotates far enough up its potential well towards the blocking triptycene arm (**12b**). This gives a tethered state **13a**, for which rotation over the barrier to **13b** is an exergonic process that occurs under thermal activation. Finally, the urethane linker can be cleaved to give the original molecule with the components rotated by 120° with respect to each other (**11b**).

Carter, N. J., & Cross, R. A. (2005). Mechanics of the kinesin step. *Nature*, *435*(7040), 308–312.

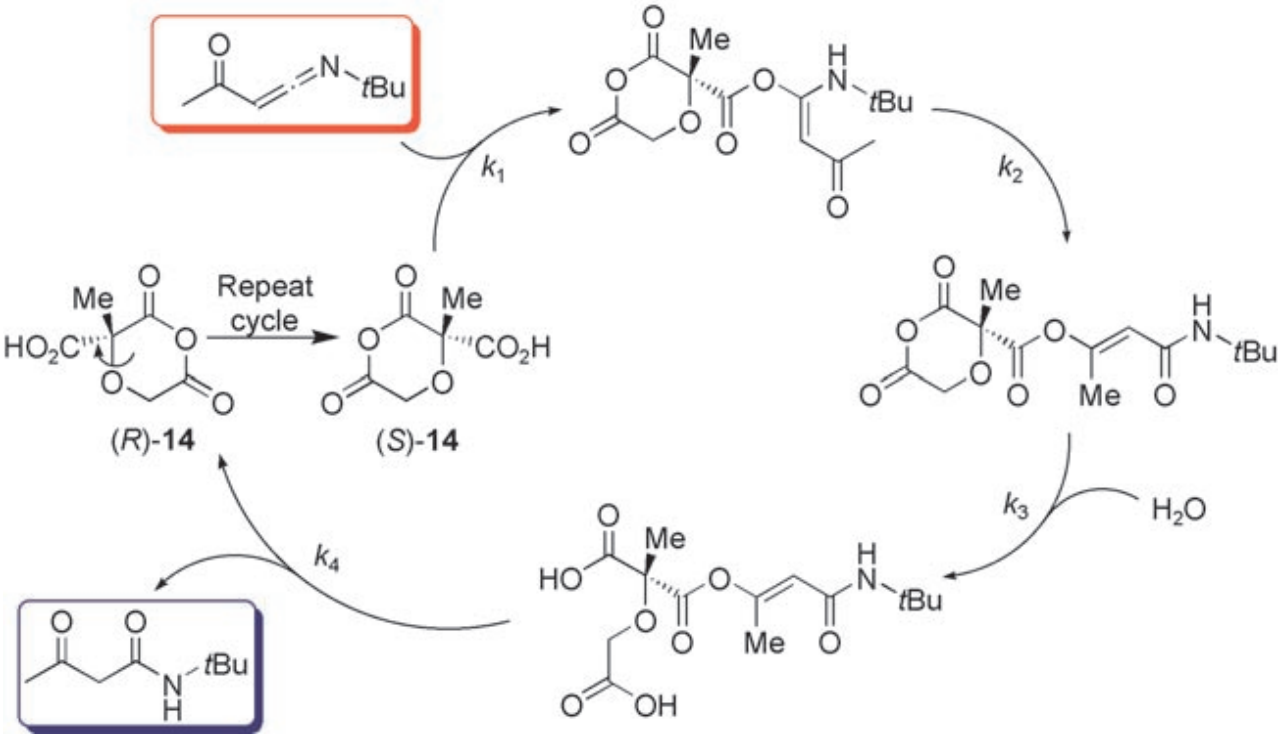

Scheme 4. Proposed system for chemically driven directional 180° rotary motion fueled by hydration of a ketenimine (red box).[77] For clarity, the catalytic cycle for a single enantiomer of motor **14** is shown. This cycle produces the opposite enantiomer, which undergoes an analogous cycle in which rotation must be biased in the opposite direction. A number of potential side reactions (not illustrated) which would divert the system from the catalytic cycle were found to be kinetically insignificant under the reaction conditions employed.

Carter, N. J., & Cross, R. A. (2005). Mechanics of the kinesin step. *Nature*, *435*(7040), 308–312.

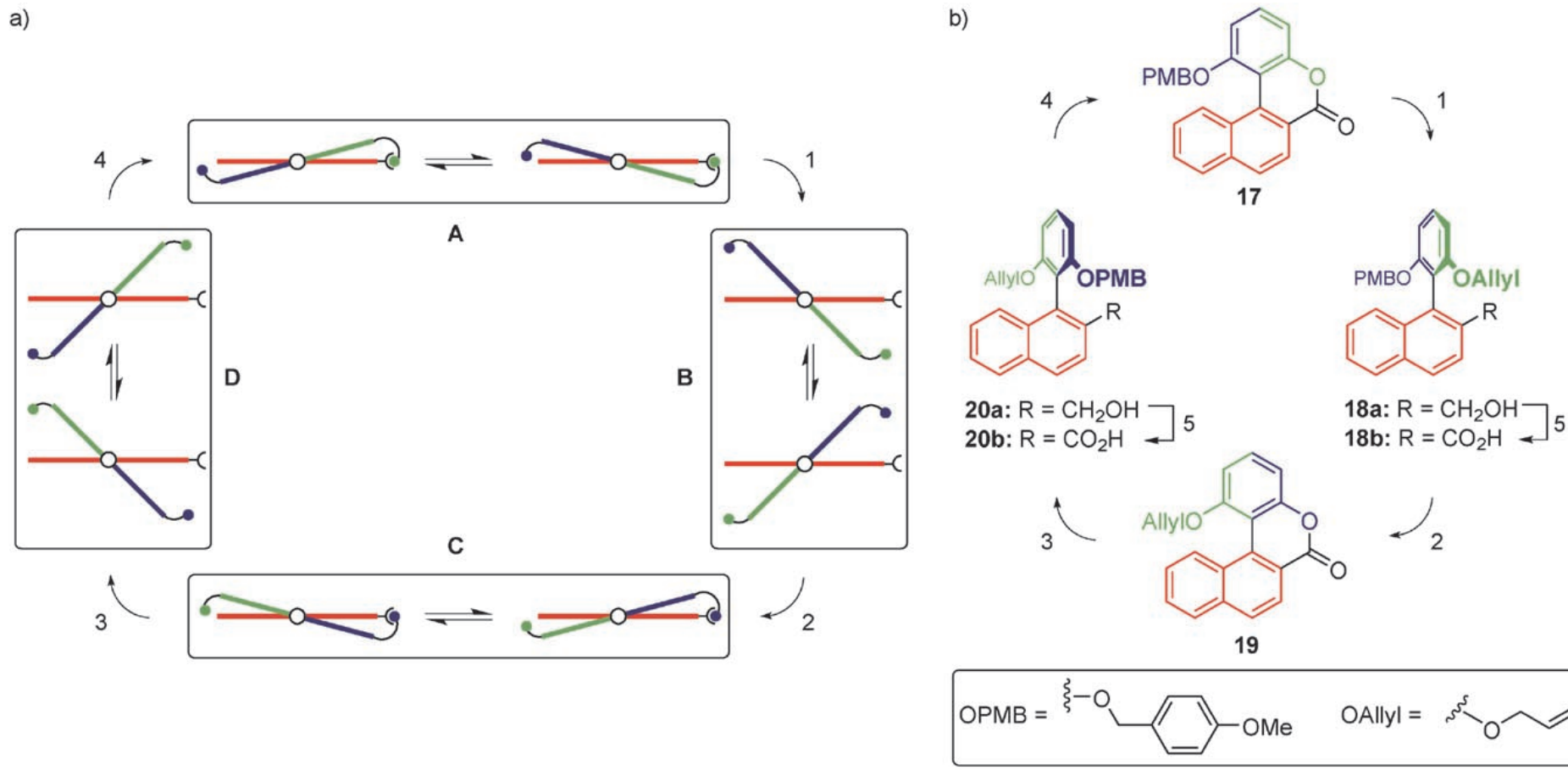

Figure 13. a) Schematic representation of unidirectional rotation around a single bond, through four states.[81] In states **A** and **C** rotation is restricted by a covalent linkage, but the allowed motion results in helix inversion. In states **B** and **D** rotation is restricted by nonbonded interactions between the two halves of the system (red and green/blue). These forms are configurationally stable. The rotation relies on stereospecific cleavage of the covalent linkages in steps (1) and (3), then regiospecific formation of covalent linkages in steps (2) and (4). b) Structure and chemical transformations of a unidirectional rotor. Reactions: 1) Stereoselective reduction with (*S*)-CBS then allyl protection. 2) Chemoselective removal of the PMB group resulting in spontaneous lactonization. 3) Stereoselective reduction with (*S*)-CBS then protection with a PMB group. 4) Chemoselective removal of the allyl group resulting in spontaneous lactonization. 5)Oxidation to carboxylic acid.

Carter, N. J., & Cross, R. A. (2005). Mechanics of the kinesin step. *Nature*, *435*(7040), 308–312.

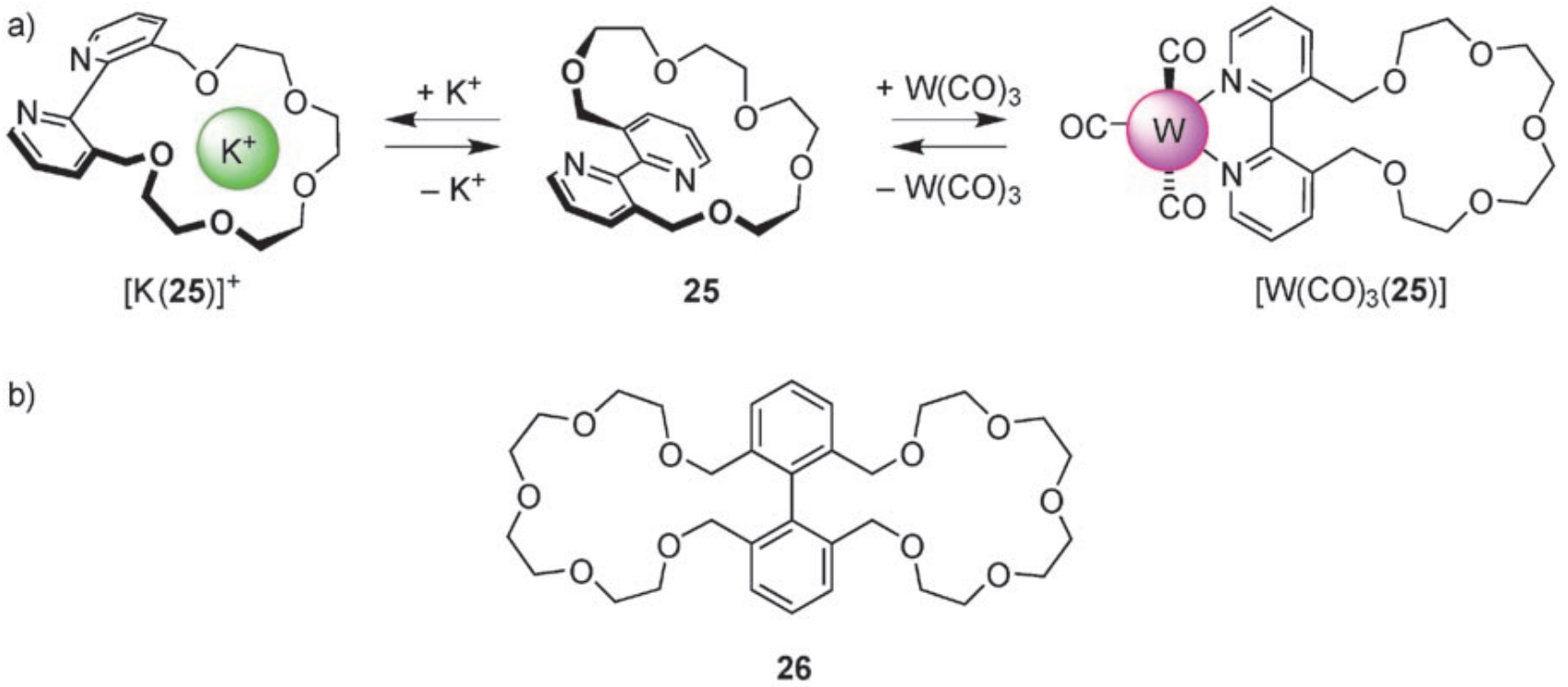

Scheme 9. a) Negative heterotropic allosteric receptor **25** binds alkali metal ions, with selectivity for K^+.[100] Chelation of tungsten to the bipyridyl moiety forces this unit to adopt a rigid conformation in which the 3 and 3′ substituents are brought close together. The resulting conformation of the crown ether does not favor binding through all the oxygen atoms and so affinity for K^+ ions is reduced. In fact [$W(CO)_3$(**25**)] shows a preference for binding the smaller Na^+ ion. b) Positive homotropic allosteric receptor **26**.[101]

Carter, N. J., & Cross, R. A. (2005). Mechanics of the kinesin step. *Nature*, *435*(7040), 308–312.

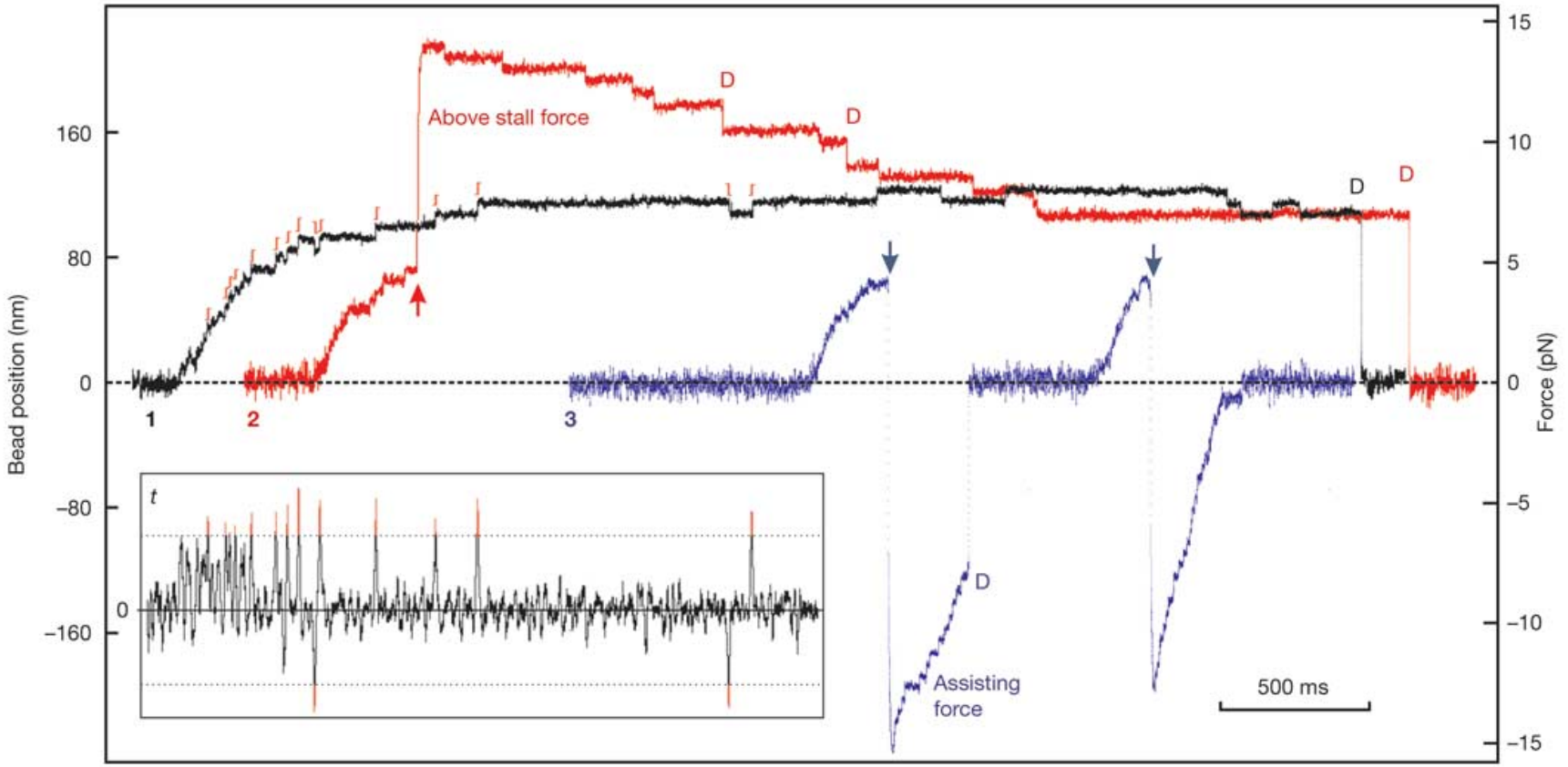

Figure 1 | **Example optical trapping records.** Three superimposed records showing the movement of single kinesin molecules towards stall force, over time. In record 1 (black), the trap and microtubule remain fixed throughout, and the kinesin walks with 8-nm steps away from the trap centre (dashed line) to stall force and finally detaches. In record 2 (red), on reaching 4 pN the microtubule is moved rapidly (upward arrow), pulling the kinesin to about 14 pN force. In some instances the kinesin responds with processive backward steps to stall force (7–8 pN). More commonly at forces above 10 pN, the kinesin would detach after a few or no backward steps, the bead returning to trap centre. Record 3 (blue) shows the opposite procedure. On reaching the 4-pN trigger force, the microtubule is quickly moved (downward arrows) to apply a large negative (assisting) force to the kinesin. Two successive experiments on the same molecule are shown. For automated dwell time calculations and step-averaging, a *t*-test step finder was applied to the bead position data. The inset shows the *t*-test profile for the first part of record 1. Steps are defined where the *t*-value exceeds a preset threshold value (dotted line). The located steps are shown offset just above record 1. In all records, detachment events (steps larger than 12 nm recognized by the step finder) are marked with D. Conditions: single kinesin molecules on 560-nm polystyrene beads, 1 mM ATP. The trap stiffnesses for the beads in these records were 0.064, 0.067 and 0.064 pN nm^{-1}, respectively. The force scale represents a trap stiffness of 0.065 pN nm^{-1}. Stage movements (arrows) were typically complete within 200 ms. The data shown are 1-ms boxcar filtered.

Carter, N. J., & Cross, R. A. (2005). Mechanics of the kinesin step. *Nature*, *435*(7040), 308–312.

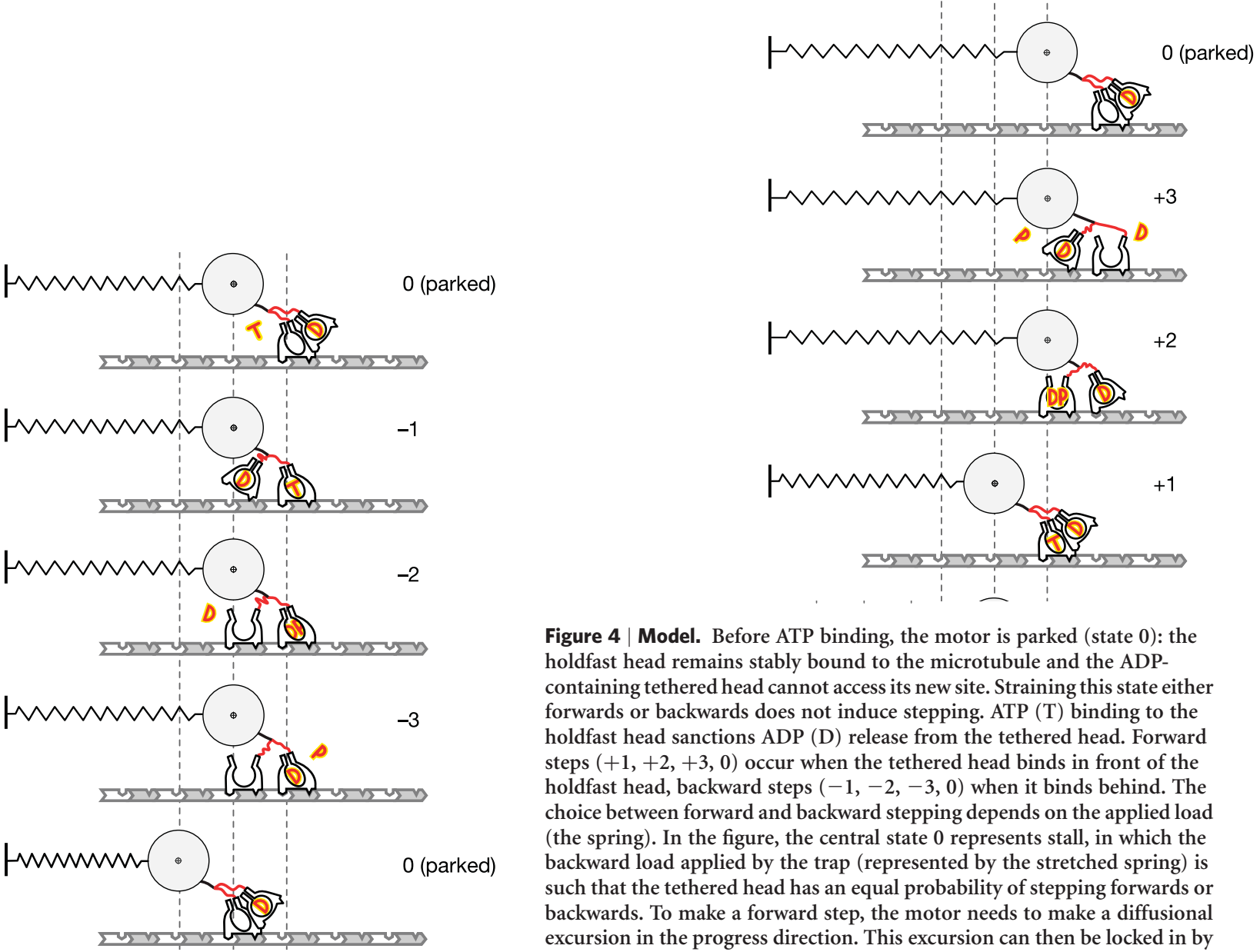

Figure 4 | Model. Before ATP binding, the motor is parked (state 0): the holdfast head remains stably bound to the microtubule and the ADP-containing tethered head cannot access its new site. Straining this state either forwards or backwards does not induce stepping. ATP (T) binding to the holdfast head sanctions ADP (D) release from the tethered head. Forward steps (+1, +2, +3, 0) occur when the tethered head binds in front of the holdfast head, backward steps (−1, −2, −3, 0) when it binds behind. The choice between forward and backward stepping depends on the applied load (the spring). In the figure, the central state 0 represents stall, in which the backward load applied by the trap (represented by the stretched spring) is such that the tethered head has an equal probability of stepping forwards or backwards. To make a forward step, the motor needs to make a diffusional excursion in the progress direction. This excursion can then be locked in by irreversible ADP release from the lead head.

Carter, N. J., & Cross, R. A. (2005). Mechanics of the kinesin step. *Nature*, *435*(7040), 308–312.

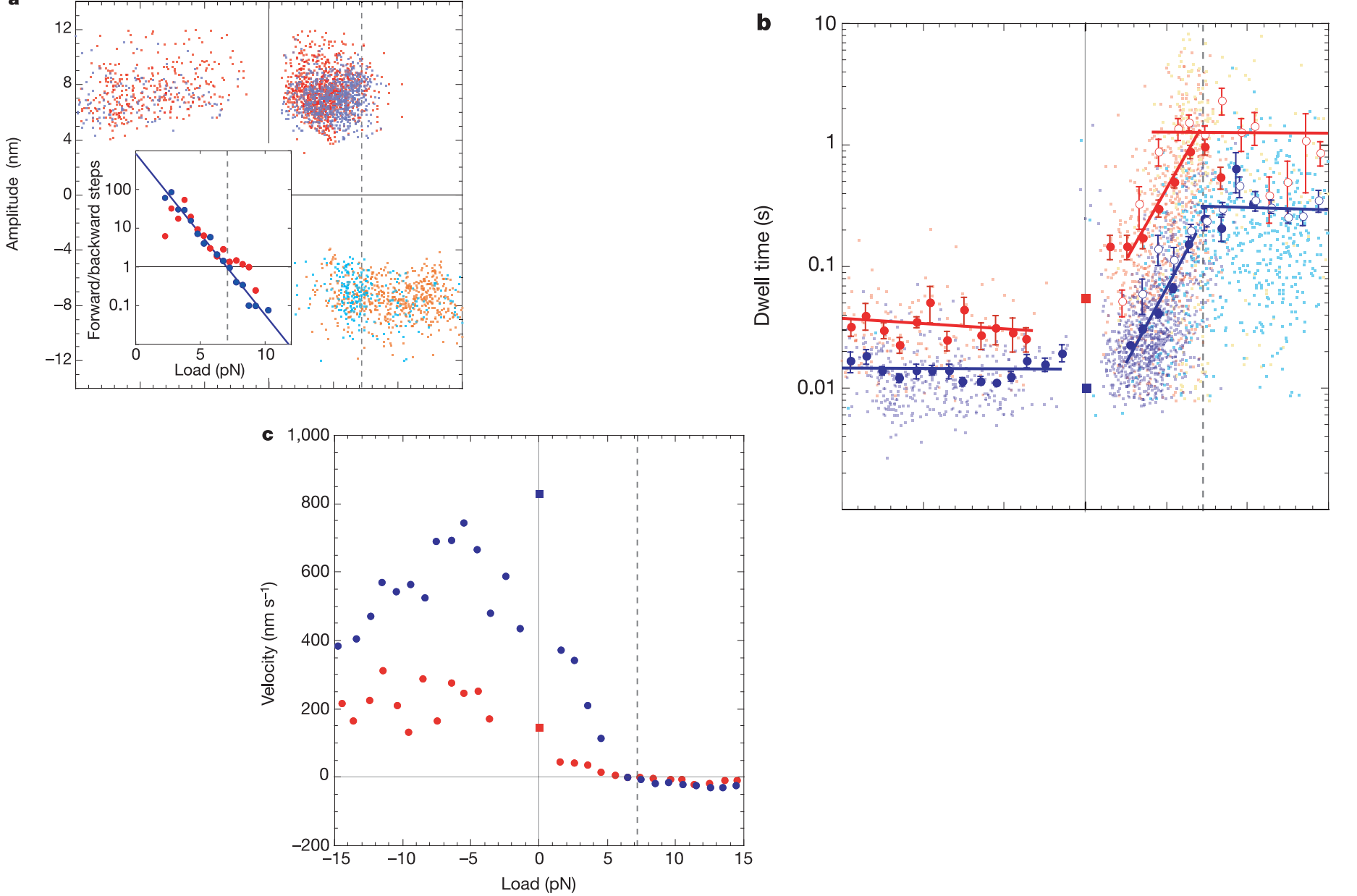

Carter, N. J., & Cross, R. A. (2005). Mechanics of the kinesin step. *Nature*, *435*(7040), 308–312.

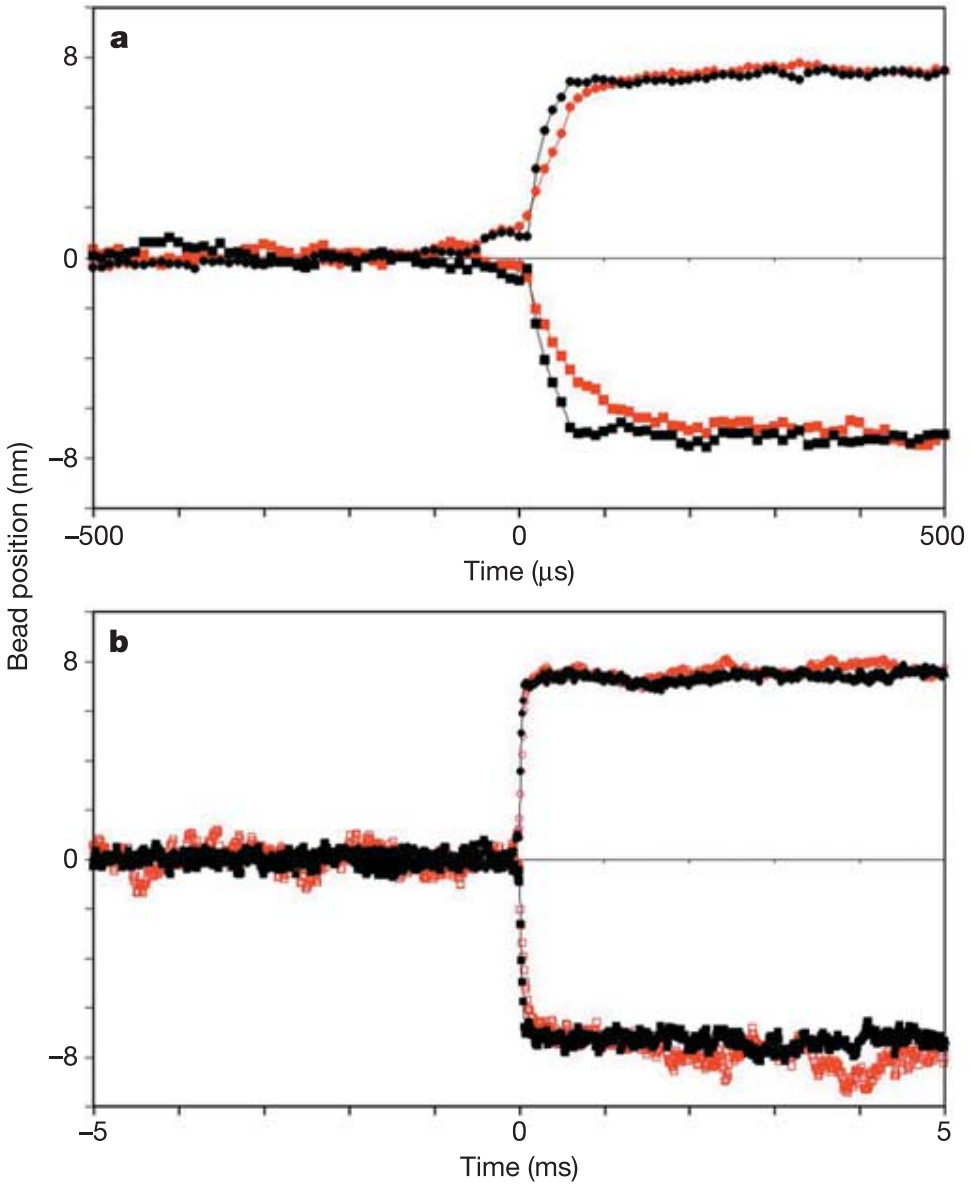

Figure 3 | **Average time course of forward and backward steps. a**, **b**, The same data sets are shown on two timescales: fine (**a**) and coarse (**b**). Step positions were determined automatically with a *t*-test step finder, followed by a least-squares exponential fit for step position refinement. The averaged forward steps (circles) and backward steps (squares) for two bead sizes are shown: the fit time constant for 500-nm beads (black) was faster than that for 800-nm beads (red). For 500-nm beads, forward steps ($n = 1{,}693$) had time constant 15.3 μs, amplitude 7.39 nm and average force 5.0 pN; for backward steps ($n = 316$) these were 19.4 μs, 7.34 nm and 6.1 pN, respectively. For 800-nm beads, forward steps ($n = 565$) had time constant 35.9 μs, amplitude 7.6 nm and force 4.7 pN; for backward steps ($n = 68$) these were 37.3 μs, 7.8 nm and 5.6 pN, respectively. All records used for the step averaging were recorded at 1 mM ATP.

Carter, N. J., & Cross, R. A. (2005). Mechanics of the kinesin step. *Nature*, *435*(7040), 308–312.

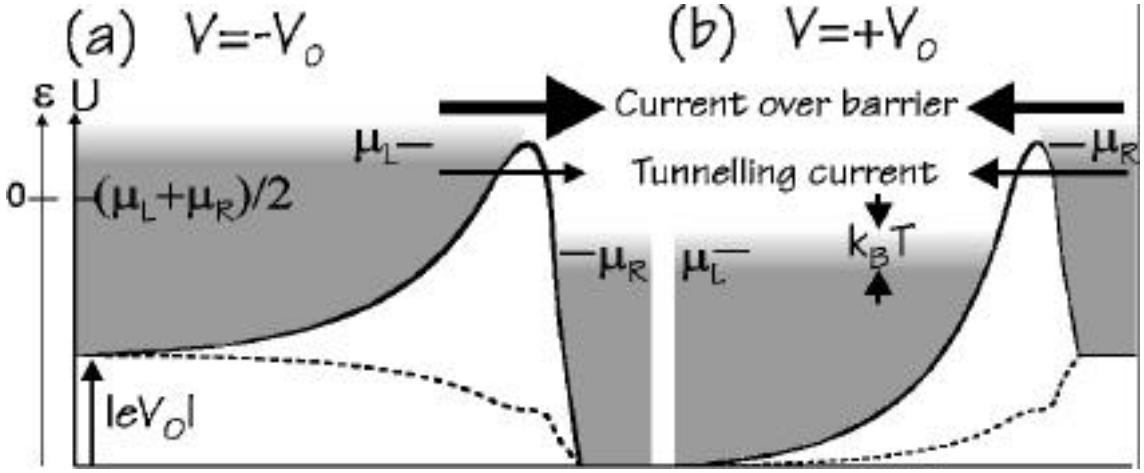

Fig 1: A rocked electron ratchet. The solid lines are an estimation of the confinement potential experienced by electrons as they traverse the experimental ratchet wave-guide shown in Fig 2 (inset). The Fermi distribution of electrons as a function of energy is indicated by the grey regions, where lighter grey corresponds to an occupation probability of less than one. The boldness of the arrows is indicative of the relative strengths of the contributions of high and low energy electrons to the current across the barrier under negative (a) and positive (b) voltages. The dashed lines indicate the spatial distribution of the assumed voltage drop over the barrier, which is scaled with the local potential gradient of the barrier at zero voltage.

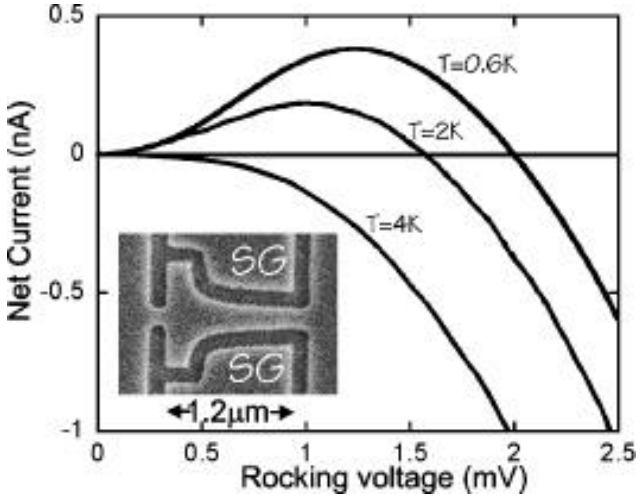

Fig. 2: Main: Measured net current as a function of rocking amplitude at a number of temperatures as indicated. Reversals in the direction of the net current as a function of rocking amplitude, and implicitly as a function of temperature, are observed. Data taken from [6]. **Inset:** A scanning electron microscope image of the ratchet device (top view). The dark regions are etched trenches that electrically deplete a two-dimensional electron gas located at the AlGaAs/GaAs interface beneath the surface, forming a one-dimensional wave-guide. Due to quantum confinement inside the waveguide, an electron moving from left to right will experience an asymmetric potential barrier similar to that shown in Fig. 1. Note the side gates (marked SG) which are used to tune the height of the potential barrier which is experienced by electrons moving though the ratchet. The left point contact does not play a significant role in the behaviour of the device as a ratchet.

Carter, N. J., & Cross, R. A. (2005). Mechanics of the kinesin step. *Nature*, *435*(7040), 308–312.

3 The Landauer model

The Landauer equation expresses the current flowing through a mesoscopic device between two reservoirs as a function of the Fermi distribution of electrons in the reservoirs and of the energy dependent probability that an electron will be transmitted through the device [7]. It may be written as:

$$I = \frac{2e}{h}\int_{-\mu_{av}}^{\infty} t(\varepsilon, V)\left[f_R(\varepsilon, V) - f_L(\varepsilon, V)\right]d\varepsilon \ , \qquad (1)$$

where

$$f_{L/R}(\varepsilon, V) = \frac{1}{1 + \exp\left(\dfrac{-\varepsilon \pm eV/2}{k_B T}\right)} \qquad (2)$$

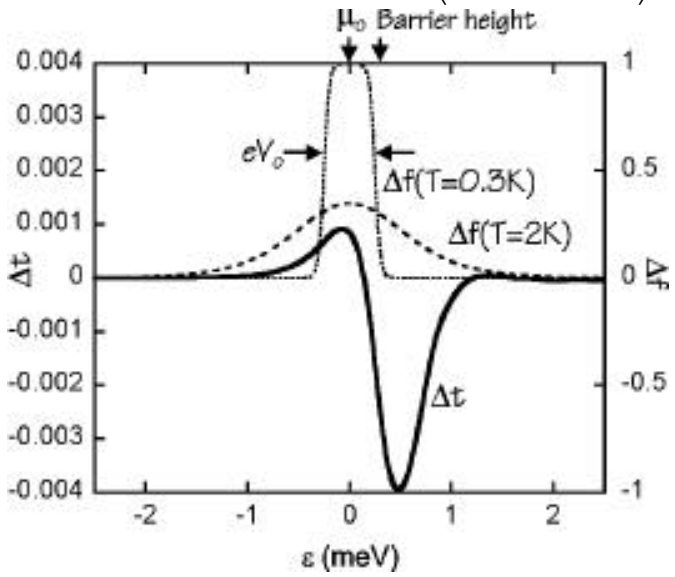

Fig. 3: The bold curve (corresponding to the left vertical axis) is the difference between the transmission probabilities for +0.5mV and –0.5mV tilting voltages as a function of electron energy. The dotted and dashed curves (corresponding to the right vertical axis) are the Fermi 'windows', $\Delta f(\varepsilon, V_0 = 0.5$ mV), centred on an equilibrium Fermi energy, $\mu_0 = 11.7$meV, for temperatures of 0.3K and 2K respectively. As the temperature is changed from 0.3K to 2K, note that the integral of the product of Δf and Δt will make a transition from positive to negative, leading to a reversal in the direction of the net particle current (Eq. 4). Small oscillations in Δt exist for $\varepsilon > 1$ meV.

Carter, N. J., & Cross, R. A. (2005). Mechanics of the kinesin step. *Nature*, *435*(7040), 308–312.

To obtain an intuitive understanding of the action of the ratchet as a heat pump at parameter values where the net particle current goes through zero, it is helpful to rewrite Eq. (7) as:

$$q_{L/R}^{net} = \mp\frac{1}{h}\int_{-\mu_{av}}^{\infty}\varepsilon\Delta t\Delta f d\varepsilon + \frac{1}{h}\frac{eV_0}{2}\int_{-\mu_{av}}^{\infty}\tau\Delta f d\varepsilon = \mp\frac{1}{2}\Delta E + \frac{1}{2}\Omega \qquad (8)$$

Here $\tau(\varepsilon, V_0) = (1/2[t(\varepsilon, +V_0) + t(\varepsilon, -V_0)])$ is the average transmission probability for an electron under positive and negative bias voltage. $\Delta E = q_L^{net} - q_R^{net}$ is the heat pumped from the left to the right sides of the device due to the energy sorting properties of the ratchet, and can be non-zero only for asymmetric barriers. $\Omega = (V_0/2)[|I(+V_0)| + |I(-V_0)|]$ is the ohmic heating, averaged over one cycle of rocking. ΔE can be interpreted as the heat pumping power of the ratchet, averaged over a period of rocking, while $\Omega = q_L^{net} + q_R^{net}$ is the electrical power input, averaged over a period of rocking. We therefore define a coefficient of performance for the ratchet as a heat pump as:

$$\chi(T, V_0) = \frac{\Delta E}{\Omega} = \frac{q_R^{net} - q_L^{net}}{q_R^{net} + q_L^{net}} \qquad (9)$$

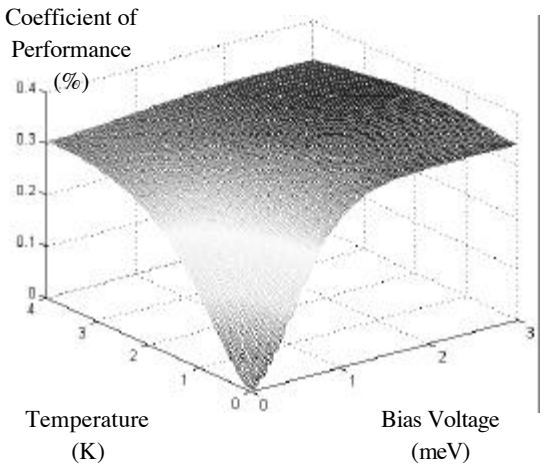

Fig. 4: The heat-pumping coefficient of performance of the ratchet model shown in Fig. 1, plotted as a function of rocking voltage and temperature. Each point on the surface corresponds to a set of values of rocking voltage, temperature and Fermi energy for which the net particle current goes through zero.

Carter, N. J., & Cross, R. A. (2005). Mechanics of the kinesin step. *Nature*, *435*(7040), 308–312.

4 Energy current

The heat change associated with the transfer of one electron to a reservoir with chemical potential μ is given by [10]:

$$\Delta Q = \Delta U - \mu \tag{5}$$

The heat current entering the left and right reservoirs associated with the particle current generated by a voltage V across the device is then obtained from the equation for the electrical current (Eq. 1). This is done by replacing the electron charge, $-e$, by a factor of $\Delta Q_{L/R}$ inside the integral. The heat current can then be written as

$$q_{L/R} = \mp\frac{2}{h}\int_{-\mu_{av}}^{\infty}(\varepsilon \pm eV/2)t(\varepsilon,V)\Delta f(\varepsilon,V)d\varepsilon \tag{6}$$

The *net* heat current into the left and right reservoirs over a full cycle of square-wave rocking, $q_{L/R}^{net} = (1/2)\left[q_{L/R}(V_0) + q_{L/R}(-V_0)\right]$, is then:

$$q_{L/R}^{net} = \mp\frac{1}{h}\int_{-\mu_{av}}^{\infty}\left[(\varepsilon \pm eV_0/2)t(\varepsilon,+V_0)\Delta f(\varepsilon,+V_0) + (\varepsilon \mp eV_0/2)t(\varepsilon,-V_0)\Delta f(\varepsilon,-V_0)\right]d\varepsilon \tag{7}$$

To obtain an intuitive understanding of the action of the ratchet as a heat pump at parameter values where the net particle current goes through zero, it is helpful to rewrite Eq. (7) as:

$$q_{L/R}^{net} = \mp\frac{1}{h}\int_{-\mu_{av}}^{\infty}\varepsilon\Delta t\Delta f d\varepsilon + \frac{1}{h}\frac{eV_0}{2}\int_{-\mu_{av}}^{\infty}\tau\Delta f d\varepsilon = \mp\frac{1}{2}\Delta E + \frac{1}{2}\Omega \tag{8}$$

Carter, N. J., & Cross, R. A. (2005). Mechanics of the kinesin step. *Nature*, *435*(7040), 308–312.